State of the Art and Present Trends in Nonlinear Microwave CAD Techniques

VITTORIO RIZZOLI, MEMBER, IEEE, AND ANDREA NERI

(Invited Paper)

Abstract—**The paper presents a survey of modern nonlinear CAD techniques as applied to the specific field of microwave circuits. A number of fundamental aspects of the nonlinear CAD problem, including simulation, optimization, intermodulation, frequency conversion, stability, and noise, are addressed and developed. For each one it is shown that either well-established CAD solutions are available, or at least a solution approach suitable for implementation in a general-purpose CAD environment can be outlined. Also, the discussion shows that the various subjects are not just separate items, but rather can be chained in a strictly logical sequence. Finally an elementary treatment of vector processing is given, to show that supercomputers can handle the involved large-size numerical problems in a most efficient way.**

I. INTRODUCTION

THIS PAPER surveys the application of computer-aided techniques to the problem of nonlinear microwave circuit simulation for engineering purposes.

For years, the general topic of nonlinear networks has been a favorite among circuit theorists, as is clearly shown by the large amount of related technical literature. As an example, a search in the INSPEC data base revealed no less than 4000 papers devoted to this subject in the last eight years. More recently the interest in nonlinear circuit techniques has begun to spread inside the microwave community, so that at present one or more nonlinear sessions usually show up in the technical programs of all major microwave meetings. The reasons for this increasing popularity are not difficult to understand, and are closely linked to the advance of microwave technology.

One first obvious aspect is that the ever-increasing miniaturization of microwave circuits, with reduced ability to trim, calls for more powerful and general design capabilities. In this respect, nonlinear circuit CAD may be essentially viewed as the extension of classic CAD to problems that have traditionally been treated by semiempirical approaches.

There is, however, another aspect, which is more promising, though more projected into the future. The maturation and spread of MMIC technology are facing us with a dramatic evolution of the traditional concepts of circuits and systems, which tend to be identified as long as more and more interconnected subsystems tend to merge into a single chip. At the same time it becomes increasingly difficult, if possible at all, to treat subsystems as individual items that can be separately specified and designed. Not surprisingly, a major impulse to the development of monolithic gallium arsenide circuits is being given by systems firms. In order to be useful, CAD techniques must obviously keep pace with technological reality, which means that conventional circuit-oriented CAD must evolve into modern system-oriented CAD. This involves the need for nonlinear capabilities, since system performance always requires nonlinear functions, and the ability to deal with very large size problems. From this viewpoint, nonlinear circuit CAD marks an essential step toward the technological update of computer-aided techniques.

In the authors' opinion, this clearly establishes the present trends in nonlinear microwave CAD. On the one hand, we have the circuit design problem, an intriguing one with several interrelated aspects, a tentative list of which is given below:

- analysis (simulation) of a known circuit;
- optimization of a nonlinear circuit;
- multiple-frequency excitation (intermodulation);
- frequency conversion (mixing);
- stability analysis;
- noise analysis.

Some of these are very popular, while others have seldom been touched on in the technical literature. What the paper tries to do in this respect is to show that the state of the art of nonlinear microwave CAD allows us to envisage a complete set of software tools covering all these aspects within the framework of a substantially unique philosophy. These tools are truly general-purpose in the CAD sense,

Manuscript received February 25, 1987; revised August 31, 1987. This work was supported by the Italian Ministry of Public Education and by the Istituto Superiore delle Poste e delle Telecomunicazioni (ISPT). The development of vectorized software tools for nonlinear microwave circuit CAD is currently being pursued as a joint research effort by the Electronics Department of the University of Bologna, Fondazione Ugo Bordoni, and Fondazione Guglielmo Marconi. This paper was first given as an invited presentation at the Workshop on Trends in Microwave CAD, held in conjunction with the 1986 IEEE MTT-S International Microwave Symposium (Baltimore, MD, June 5, 1986).

V. Rizzoli is with the Dipartimento di Elettronica, Informatica e Sistemistica, University of Bologna, Villa Griffone, 40044 Pontecchio Marconi, Bologna, Italy.

A Neri is with the Fondazione Ugo Bordoni, Roma, Italy.

IEEE Log Number 8718989.

which means there are no restrictions on circuit topologies, device representations, or electrical functions. To a certain extent this requires some anticipation, since some of the problems already have well-established solutions, while others are still at the stage of conceptual development.

On the other hand, the extension of circuit CAD to cover system requirements may be expected to introduce at least one major new difficulty, that is, the very large size of the related numerical problems. This may arise both from the complexity of circuit topologies including several interacting subsystems, and from the need to deal with broad frequency spectra, possibly encompassing the MHz as well as the GHz regions. In this respect, we try to demonstrate that a key tool for the solution of this additional problem can be provided by one of the best-known concepts of modern computer science, namely parallel processing, and by its most common present-day implementation, represented by supercomputers. Supercomputers have the potential of extending to the nonlinear CAD domain all of the design issues that are now commonplace in linear CAD, and of making them as handy as their linear counterparts.

Of course, for this to become possible, all aspects of the general simulation problem should be consistently developed, especially passive and active device modeling. However, this paper is not going to touch on such aspects since they are covered by specialized presentations in this same issue, but rather will be devoted to methodology.

II. Simulation

The simulation of nonlinear circuits is by far the most popular aspect of the entire job. Considerable effort and considerable ingenuity have been spent in devising new nonlinear analysis methods or improvements to existing ones. During the 15th European Microwave Conference, in Paris, an entire tutorial session was devoted to this subject [1]; thus to avoid duplications as far as possible, only a schematic classification and a brief highlight of some of the best-known approaches will be reported here.

In Table I a number of analysis algorithms are organized according to the type of description they adopt for the two fundamental kinds of circuit components, the linear and the nonlinear ones. Attention here is restricted to those methods that we could name "quasi-exact," i.e., that address the problem in a rigorous way except for numerical approximation, and do not rely upon *a priori* limiting assumptions such as weak nonlinearity or almost-monochromatic operation.

TABLE I
Quasi-Exact Analysis Approaches

LINEAR COMPONENTS DESCRIPTION		NONLINEAR COMPONENTS DESCRIPTION: TIME DOMAIN	NONLINEAR COMPONENTS DESCRIPTION: FREQUENCY DOMAIN
TIME DOMAIN		DIRECT INTEGRATION SHOOTING METHODS EXTRAPOLATION METHODS	
FREQUENCY DOMAIN		HARMONIC BALANCE SYSTEM SOLVING OPTIMIZATION CONTINUATION METHODS RELAXATION METHODS SAMPLE BALANCE	POWER SERIES

A. Time-Domain Methods

A huge amount of technical literature is available on the general topic of nonlinear circuit simulation in the time domain, concerning both theoretical and computational aspects. Generally speaking, this work is not oriented toward microwave applications; thus it is beyond the scope of this paper to survey it. For the present purposes it will be sufficient to quote a number of special issues of the IEEE Transactions on Circuits and Systems [2]–[5], where several review papers and a very extensive bibliography on the subject can be found. In particular, a review of the best-known time-domain simulation programs is given in [6].

A specific effort aimed at the extension of time-domain techniques to cover microwave applications is currently being made by several research groups [7]–[13]. An example of a microwave-oriented time-domain computational scheme is briefly outlined below. The use of suitable models of nonlinear capacitors and inductors leads to an equivalent circuit containing resistors and controlled sources as the only nonlinear components [13]. The circuit may thus be described in terms of a state vector of capacitor voltages, inductor currents, voltages at the transmission-line ports, and nonlinear resistor control variables. Combining Kirchhoff's laws with the voltage–current relationships of the circuit components results in the following set of coupled differential–difference and algebraic equations with constant coefficients:

$$\begin{aligned} \frac{d\boldsymbol{x}_1}{dt} &= \boldsymbol{A}_1\boldsymbol{x} + \boldsymbol{B}_1\boldsymbol{u} + \boldsymbol{C}_1\frac{d\boldsymbol{u}}{dt} \\ \boldsymbol{x}_2 &= \boldsymbol{A}_2\boldsymbol{x}(t-T_t) + \boldsymbol{B}_2\boldsymbol{u}(t-T_t) \\ 0 &= \boldsymbol{A}_{31}\boldsymbol{x}_1 + \boldsymbol{A}_{32}\boldsymbol{x}_2 + \boldsymbol{B}_3\boldsymbol{u} + \boldsymbol{F}(\boldsymbol{x},\boldsymbol{u},t) \\ \boldsymbol{y} &= \boldsymbol{A}_4\boldsymbol{x} + \boldsymbol{B}_4\boldsymbol{u} + \boldsymbol{C}_4\frac{d\boldsymbol{u}}{dt} \end{aligned} \tag{1}$$

where

$\boldsymbol{x}_1$ vector of lumped state variables,
$\boldsymbol{x}_2$ vector of distributed state variables,
$\boldsymbol{x}_3$ vector of nonlinear resistor control variables,
$\boldsymbol{x}$ overall state vector,

A, B, C	time-independent circuit matrices,
u	source vector,
T_i	transmission-line delays,
F	vector of nonlinear resistor characteristics,
y	output vector.

The system (1) is directly solved in the time domain by a suitable integration scheme [14], [15], requiring the solution of a set of nonlinear algebraic equations at each iterative step. The starting point is usually chosen as the result of a dc analysis.

Apparently, methods that work entirely in the time domain should represent the most natural and straightforward approach to the simulation problem. As a matter of fact, real-world circuits do work in the time domain, and semiconductor devices are naturally described in the time domain, too. However, such methods generally suffer from two major inconveniences. First of all, the only available means of accurately computing and measuring linear microwave components is to work in the frequency domain under sinusoidal excitation, except of course for elementary ones. Thus the difficulties come from the time-domain analysis of the linear subnetwork whenever realistic component models are to be dealt with. For instance, the description of a device as simple as a microstrip line with frequency-dependent propagation constant and characteristic impedance still represents a problem in the time domain. Of course, in principle one could think of such approaches as frequency-domain to time-domain conversions and convolution integrals [16], [17], but the practical feasibility of this still has to be demonstrated. The second point is numerical efficiency. An analysis based on the direct integration of the time-domain network equations would typically spend most of its computational effort on transient evaluation, while most of the user's interest is concentrated on steady-state information. To give a representative idea of what this means quantitatively, let us consider, for instance, some of the numerical results presented in [12]. Fig. 3 of this paper shows that the analysis of a circuit as simple as a biased FET without anything else requires the consideration of at least ten RF periods to reach steady state when using SPICE, one of the best-known time-domain simulators [18]. Similar conclusions are reached in [19]. Also, the situation may be definitely worse for more complicated circuits, not to mention special cases involving high-Q components, such as dielectric resonators.

For this reason, considerable effort has been spent by circuit theorists in devising techniques allowing the calculation of the transient to be at least partially bypassed and the steady state to be reached quickly. The basic concept is usually the evaluation of a set of initial conditions from which the network starts in periodic steady state. The so-called shooting methods [20]–[23] consist of a direct search for such initial conditions by a Newton iteration or some other nonlinear optimization technique. An alternative approach is to compute the state of the circuit at a number of instants by time-domain integration, and then to extrapolate from these by algebraic methods the state from which the network starts in time-periodic regime [24]. We limit ourselves to this brief mention because the application of these approaches to microwave circuits has been only marginal.

A limiting form of the same ideas is represented by those methods that completely disregard the transient and directly focus on the steady state. The physical unknowns of the problem are still represented by state-variable waveforms, but the formulation is such that these waveforms are *a priori* guaranteed to be time-periodic. For numerical purposes the waveforms are approximately described by a discrete set of scalar unknowns; if the discretization is carried out in the frequency domain this leads to harmonic-balance methods.

B. Harmonic-Balance Techniques

A quick review of the fundamentals of this approach is worthwhile because of the key role it plays in modern nonlinear CAD techniques. The network is first decomposed into a linear and a nonlinear multiport subnetwork having the same number of ports, n_D. The subdivision criterion usually represents a tradeoff between two opposite needs: on the one hand, n_D should be kept to a minimum for optimum numerical efficiency, while on the other, increasing the number of ports usually makes for an easier description of the nonlinear subnetwork.

The latter is represented by a set of time-domain nonlinear equations. Although this can be done in a number of ways, for the sake of generality and for later convenience we shall make use of the following system of parametric equations:

$$v(t) = \phi\left[x(t), \frac{dx}{dt}, \cdots \frac{d^n x}{dt^n}\right]$$
$$i(t) = \psi\left[x(t), \frac{dx}{dt}, \cdots \frac{d^n x}{dt^n}\right] \tag{2}$$

where v and i are vectors of instantaneous voltages and currents at the nonlinear subnetwork ports, and x is a set of time-dependent quantities used as state variables. ϕ and ψ are nonlinear and analytically or numerically known.

The linear subnetwork is described in the frequency domain. For maximum generality its equations are written in the form

$$A(\omega)V(\omega) + B(\omega)I(\omega) + D(\omega) = 0 \tag{3}$$

where A and B are circuit matrices, V and I are vectors of voltage and current phasors at the network ports, and D is a set of driving functions. For a well-conditioned network all vector quantities appearing in (2) and (3) have the same size n_D.

In steady state, the state-variable waveforms are approximated by

$$x(t) = \sum_{k=-N_H}^{N_H} X_k \exp(jk\omega_0 t) \tag{4}$$

($X^*_{-k} = X_k$, $*$ = complex conjugate), where ω_0 is the

fundamental angular frequency of the time-periodic regime. Thus the steady state is completely identified by the vector $\boldsymbol{X}$ of all $\boldsymbol{X}_k$'s (state vector).

The circuit analysis problem now consists of finding the state vector $\boldsymbol{X}$ in such a way that the time-domain voltages and currents obtained from (2) through (4) have spectral components satisfying (3) at $\omega = k\omega_0$ $(0 \leqslant k \leqslant N_H)$. Making use of the fast Fourier transform, one obtains the nonlinear solving system

$$\boldsymbol{E}(\boldsymbol{X}) = 0 \tag{5}$$

where the kth subvector of $\boldsymbol{E}$, namely

$$\boldsymbol{E}_k(\boldsymbol{X}) = \boldsymbol{A}(k\omega_0)\boldsymbol{\Phi}_k(\boldsymbol{X}) + \boldsymbol{B}(k\omega_0)\boldsymbol{\Psi}(\boldsymbol{X}) + \boldsymbol{D}(k\omega_0) \tag{6}$$

$(0 \leqslant k \leqslant N_H)$ is a set of harmonic-balance errors at $k\omega_0$. Note that (5) is equivalent to a system of

$$N = n_D(2N_H + 1) \tag{7}$$

real equations in as many real unknowns. Thus for a forced or nonautonomous circuit, the problem is well posed from a mathematical viewpoint. For an autonomous circuit of given topology ($\boldsymbol{D}(k\omega_0) = 0$ for $k \neq 0$, $\boldsymbol{A}$, $\boldsymbol{B}$ *a priori* assigned), only dc solutions will exist in general. Nonstatic solutions may, of course, exist for some values of the fundamental, so that ω_0 must be regarded as an additional real unknown in (5). As a consequence, one of the remaining real unknowns (e.g., the phase of one of the harmonics) may be arbitrarily chosen, and the electrical regime is invariant with respect to a shift of the time origin. Note, however, that this situation is somewhat unusual in microwave engineering practices: most often one is faced with oscillator *design* problems whereby ω_0 is *a priori* fixed as a design goal. The required degree of freedom must then be available under the form of a free circuit parameter, so that the problem becomes one of circuit optimization from the CAD viewpoint (see Section III).

The method outlined above is known as the "piecewise" harmonic-balance technique [25], and has the advantage that the required number of state variables is equal to the number of linear subnetwork ports, no matter what the actual number of lumped or distributed reactive components. Thus the problem size is considerably reduced with respect to time-domain techniques and to earlier implementations of the harmonic-balance concept [26]. As an alternative to the piecewise harmonic-balance technique, a nodal analysis approach has also been proposed in [27]. The same reference also provides an in-depth review of harmonic-balance concepts.

Note that the harmonic-balance method takes advantage of the most accurate and straightforward approach to the simulation of both linear and nonlinear circuit components.

Harmonic-balance techniques have been used very extensively in the technical literature to analyze virtually any kind of nonlinear microwave subsystem. Most applications are based on the general guidelines presented above, except for minor details. On the other hand, a number of different strategies have been developed in order to solve numerically the system (5). Some of these deserve a brief discussion because of their conceptual importance and widespread acceptance.

1) Direct Methods: The conceptually simplest way to solve the problem is to directly apply to (5) any numerical system-solving algorithm. Such solution routines are available in virtually all mathematical libraries (e.g., CERN, IMSL). For well-behaved circuits (e.g., weakly nonlinear), a simple Newton iteration is often sufficient to quickly achieve convergence: this is usually the case for circuits containing only FET's as the active elements.

As a more robust, but less efficient, alternative [28], one can use a nonlinear optimization scheme to minimize the objective function

$$E(\boldsymbol{X}) = \|\boldsymbol{E}(\boldsymbol{X})\| \tag{8}$$

representing a combined harmonic-balance error ($\|\ \|$ indicates the norm). Of course, some care must be taken in choosing the numerical algorithm. In the user-oriented CAD perspective, it is absolutely mandatory that the analysis algorithm be able to reach convergence starting from initial values automatically set by the program in a conventional way; this means that there is no starting-point information available. An effective though obvious way to obtain this result is to approach the solution by a direct search scheme and then to refine it by a Newton iteration. Excellent results have been reached by Powell's method [29]. Quasi-Newton methods [30] also yield satisfactory performance: in a sense they represent a different implementation of the same concept, since they also rely upon a combination of one-dimensional searches and gradient iterations. The starting point may be just taken as zero for nonautonomous circuits; for self-oscillating networks it is usually better to initially set to a suitable nonzero value the magnitude of the harmonic that most directly affects the circuit output power. This has the effect of avoiding the static solution, which generally exists in the autonomous case.

2) Continuation Methods: Convergence of direct iterative approaches may sometimes be improved by continuation methods [31], which have been successfully applied to nonlinear microwave circuit problems by several authors [32]–[35]. In this case, the original problem (5) is replaced by an auxiliary one of the form

$$\boldsymbol{F}(\boldsymbol{X}, \rho) = 0 \tag{9}$$

where $\boldsymbol{F}$ is continuously dependent on a parameter ρ. The auxiliary problem (9) is defined in such a way that a solution $\boldsymbol{X}^0$ is known for a certain value, say 0, of the continuation parameter, and that the original problem is reobtained for a different value, say 1. Thus

$$\boldsymbol{F}(\boldsymbol{X}^0, 0) = 0$$
$$\boldsymbol{F}(\boldsymbol{X}, 1) = \boldsymbol{E}(\boldsymbol{X}). \tag{10}$$

The required solution $\boldsymbol{X}$ can now be generated starting from the known vector $\boldsymbol{X}^0$ by a step-by-step mechanism, through a sequence of intermediate solutions corresponding to increasing values of ρ. Each intermediate step is

obtained by solving a nonlinear problem which is very well conditioned, because its starting point and solution can be made as close as desired by making correspondingly small the step of the continuation parameter. Multiple solutions can be found by extending the generation of the solution curve beyond the first operating point, of course in the case where the curve itself bends back towards the $\rho = 1$ position. Very sophisticated algorithms available in the literature allow the path to be followed across the turning points [36].

It is not easy to establish in general whether or not the use of a continuation method does yield a consistent performance improvement with respect to the corresponding direct solution approach. The authors' experience tends to show that they are roughly equivalent from the viewpoint of computational efficiency. In principle, continuation methods guarantee that a solution can always be reached by taking sufficiently small steps of the continuation parameter, while obviously direct methods do not provide the same assurance. On the other hand, direct methods are very simple and flexible, and lend themselves nicely to the implementation of circuit optimization schemes, as will be shown later on.

In both cases, a key step for obtaining good computational efficiency is to make use of the gradient evaluation algorithm outlined below [27], [37]. This mechanism is based on the assumption that the Jacobians of the nonlinear subnetwork equations (2) with respect to the state variables and to their time derivatives are available in closed form and can be represented by Fourier expansions:

$$\frac{\partial \phi}{\partial y_m} = \sum_p \boldsymbol{C}_{m,p} \exp(jp\omega_0 t)$$
$$\frac{\partial \psi}{\partial y_m} = \sum_p \boldsymbol{D}_{m,p} \exp(jp\omega_0 t) \tag{11}$$

where $y_m = d^m x/dt^m$, $0 \leq m \leq n$. As we shall see, these expansions play an important role in the solution of the generalized mixer problem and of the related problems of stability and noise analysis. Once the coefficients $\boldsymbol{C}_{m,p}$, $\boldsymbol{D}_{m,p}$ have been found by the FFT, the Jacobians of the harmonics $\boldsymbol{\Phi}_k, \boldsymbol{\Psi}_k$ with respect to the state-variable harmonics may be expressed as [37]

$$\frac{\partial \boldsymbol{\Phi}_k}{\partial \boldsymbol{X}_s} = \sum_{m=0}^{n} (js\omega_0)^m \boldsymbol{C}_{m,k-s}$$
$$\frac{\partial \boldsymbol{\Psi}_k}{\partial \boldsymbol{X}_s} = \sum_{m=0}^{n} (js\omega_0)^m \boldsymbol{D}_{m,k-s}. \tag{12}$$

Note that all vector quantities appearing in (11), (12) have the same size n_D (i.e., the number of nonlinear subnetwork ports).

3) Relaxation Methods: As an alternative to the search strategies described above, the harmonic-balance equations may be solved by relaxation methods [40]–[45]. In the simplest approach, the vector of state variables $\boldsymbol{x}(t)$ is chosen as a set of n_D voltages or currents at the nonlinear subnetwork ports, and it is assumed that the corresponding circuit matrix of the linear subnetwork exists.

Let the complementary set of voltages and currents be denoted by $\boldsymbol{y}(t)$, and its vector of harmonics by $\boldsymbol{Y}$. The time-domain analysis of the nonlinear subnetwork by (4) and (2), and the subsequent use of the FFT then establish a relationship of the form

$$\boldsymbol{Y} = \boldsymbol{T}(\boldsymbol{X}) \tag{13}$$

where $\boldsymbol{T}$ is a (numerically defined) nonlinear vector operator. The frequency-domain equations of the linear subnetwork are now written as

$$\boldsymbol{X} = \boldsymbol{H}\boldsymbol{Y} + \boldsymbol{D} \tag{14}$$

where $\boldsymbol{H}$ is a hybrid matrix and $\boldsymbol{D}$ represents a set of driving functions ($\boldsymbol{D} \neq 0$). Combining (14) with (13) leads to the solving system

$$\boldsymbol{X} = \boldsymbol{H}\boldsymbol{T}(\boldsymbol{X}) + \boldsymbol{D} = \boldsymbol{F}(\boldsymbol{X}) \tag{15}$$

which is now formulated as a fixed-point problem of the vector nonlinear operator $\boldsymbol{F}$. This is naturally suited for a relaxation approach; if the ith estimate of the state vector is denoted by $\boldsymbol{X}^{(i)}$, the most obvious iteration scheme is defined by

$$\boldsymbol{X}^{(i+1)} = \boldsymbol{F}[\boldsymbol{X}^{(i)}]. \tag{16}$$

It is quite clear that this approach is potentially attractive because of its reduced computational cost; however, its reliability is limited because convergence cannot be *a priori* guaranteed [38].

To improve the rather poor convergence properties of the direct iteration (16), more sophisticated iteration schemes have been proposed. An effective and popular one, which was successfully applied to diode and FET circuits [40]–[42] uses the following update mechanism:

$$\boldsymbol{X}^{(i+1)} = \boldsymbol{P}^{(i)}\boldsymbol{F}[\boldsymbol{X}^{(i)}] + [\boldsymbol{1} - \boldsymbol{P}^{(i)}]\boldsymbol{X}^{(i)} \tag{17}$$

where $\boldsymbol{P}^{(i)}$ is a diagonal matrix of iteration-dependent convergence parameters, and $\boldsymbol{1}$ is an identity matrix.

Although (17) can be brought to perform much better than (16) by a suitable choice of the convergence parameters, its convergence properties still remain critically related to the specific aspects of each individual problem, and in particular to the impedance level of the nonlinear subnetwork [41]. Low impedances improve convergence when voltages are chosen as the independent variables, and conversely. This criticality can be easily inferred, for instance, from [41, fig. 6]. In this case a 5-Ω change of the nonlinear subnetwork impedance separates a condition of optimum convergence rate from one where convergence is not achieved at all. An important consequence of this situation is that the choice of the state variables is usually not free, but rather is dictated by the frequency behavior of the linear subnetwork. In turn, this implies that the time-domain analysis of the nonlinear subnetwork may require the integration of a set of differential equations

[41]. Think, for instance, of a varactor diode for which the current rather than the voltage has to be used as the state variable in order to obtain convergence. In such cases, the computational advantage of relaxation methods with respect to direct solution methods becomes questionable.

It is noteworthy that the convergence properties may be improved by resorting to even more complex iteration strategies. As an example, $x(t)$ and $y(t)$ could be defined as two independent combinations of *all* voltages and currents at the nonlinear subnetwork ports, which of course can lead to considerably increased complication in the numerical definition of the nonlinear operator $\boldsymbol{F}$. A good choice turns out to be the use of incident and reflected waves, rather than voltages and currents, as the state variables, since this takes advantage of the subunitary nature of the scattering matrix [43]. A very well known approach falling within this class is Kerr's multiple-reflection method [39].

The above discussion makes it clear that relaxation methods are not ideal candidates for general-purpose CAD applications or for nonlinear circuit optimization because of a certain lack of reliability. Furthermore, they are usually not very well suited for analyzing nonlinear circuits having multiple operating points, such as oscillators or frequency dividers. On the other hand, relaxation methods can represent an excellent choice for specialized applications, or as a backup to conventional harmonic-balance techniques in general-purpose programs.

C. Other Analysis Approaches

To conclude this brief and by necessity incomplete survey of nonlinear analysis methods, we would like to mention two other approaches that are potentially interesting, but of course do not share the maturity and widespread acceptance of the previously described ones.

One of them is referred to as the "power-series" method in Table I [45]. It is a harmonic-balance technique, but is based on a generalized power-series description of the nonlinear components [46], [47]. Once this has been developed, which is not necessarily an easy job, all required calculations may be carried out in the frequency domain, thus avoiding any time-consuming Fourier transforms.

The other one, which was arbitrarily named the "sample-balance" method in Table I, may be viewed in a sense as the dual of harmonic-balance techniques. It relies upon a direct time-domain approximation of the state-variable waveforms by suitable basis functions such as periodic cubic splines [48], [49], and uses time-domain samples as problem unknowns. The errors to be minimized are produced by comparing time-domain samples of the linear and nonlinear subnetwork responses. The linear subnetwork is analyzed in the frequency domain and its time-domain response to an elementary excitation is found once for all by Fourier transformation; at any subsequent step the time-domain response to a general driving force is simply found by linear superposition.

III. Optimization

From the general CAD viewpoint, circuit optimization obviously represents a most important goal, and a natural follow-up to the analysis problem. In the linear CAD case, the transition from the latter to the former is stepless: once a suitable analysis algorithm has been developed, this can be coupled to a minimization program—in the simplest case an off-the-shelf one—to produce an optimization-based design capability. Unfortunately this is not true in the nonlinear case, which could give a possible explanation of the striking disproportion between the considerable number of studies in the technical literature devoted to analysis methods and the sporadic attention paid to optimization. According to the authors' experience, there are a few basic reasons for this, which can be synthesized as follows.

As a first point, a full analysis of a nonlinear microwave circuit is typically too time-consuming to be effectively used as the objective-function generation mechanism within an optimization loop. A straightforward consequence is that the conventional linear optimization scheme is not applicable to nonlinear circuits: in fact, using a steady-state analysis to generate the objective function to be minimized would result is exceedingly large computer costs. Nonlinear circuit optimization thus requires the development of specialized algorithms based on the integration of the two fundamental aspects of circuit analysis and function minimization. The general rule is that the approach adopted should not require a full nonlinear analysis to be carried out at each step of the optimization loop. If we accept this viewpoint, we can go over the various analysis algorithms to understand whether or not they are potentially useful for optimization purposes. The most obvious candidates are those methods treating the analysis itself as an optimization problem, since any constraint arising from electrical specifications can be added to the objective function in a simple and straightforward way.

One of the first attempts to apply these principles in conjunction with time-domain methods, and more precisely shooting methods, was reported by Director and Wayne Current in 1976 [50]. Their approach is briefly described below. As in conventional shooting methods [20]–[23], the unknowns are a set of initial conditions from which the network starts in periodic steady state. If the vector of state variables is denoted by $x(t)$, such conditions will be represented by $x(0)$. These unknowns are now complemented by a set of linear circuit parameters, namely $\boldsymbol{p}$, so that the overall set of designable parameters is given by

$$\boldsymbol{U} = \left[\boldsymbol{x}^T(0), \boldsymbol{p}^T\right]^T \tag{18}$$

the superscript T denoting transposition. The objective function to be minimized is defined as [48]

$$F(\boldsymbol{U}) = \int_0^{T_0} \left\{ E_1[\boldsymbol{x}(t), \boldsymbol{U}, t] + E_2[\boldsymbol{x}(t), \boldsymbol{U}, t] \right\} dt \tag{19}$$

where $T_0 = 2\pi/\omega_0$ is the steady-state period. In (19), E_2

represents a suitable performance function arising from the design specifications, while E_1 has the expression

$$E_1[\boldsymbol{x}(t), \boldsymbol{U}, t] = [\boldsymbol{x}(t) - \boldsymbol{x}(0)]^T \frac{d\boldsymbol{x}}{dt} \tag{20}$$

and thus introduces the steady-state condition. The state $\boldsymbol{x}(t)$ is obtained by a time-domain integration of the usual circuit equations with starting point $\boldsymbol{x}(0)$. To solve the problem, the objective F is simultaneously minimized with respect to the whole set of unknowns $\boldsymbol{U}$.

Note, however, that this attempt was partially unable to meet its main goal, that is, the elimination of any complete steady-state nonlinear analysis within the optimization loop. In fact it was found [50] that a steady-state analysis had to be performed before every gradient evaluation of the quasi-Newton algorithm adopted. Otherwise the iteration would often converge upon a set of initial conditions that were found not to represent a steady state after running a time-domain analysis over many cycles.

This experience clearly suggests that the aforementioned optimization concepts can only be brought to a fully satisfactory implementation in conjunction with those methods that *a priori* guarantee the periodicity of the electrical regime, such as harmonic-balance techniques.

An approach to nonlinear circuit optimization based on the harmonic-balance concept is outlined below [51], [52]. This time the set of designable parameters is

$$\boldsymbol{U} = [\boldsymbol{X}^T, \boldsymbol{p}^T]^T \tag{21}$$

where $\boldsymbol{X}$ is the vector of all state-variable harmonics. The objective function arises from two contributions, one of which is the harmonic-balance error, while the other originates from the design specifications. We thus have

$$F(\boldsymbol{U}) = [\|\boldsymbol{E}(\boldsymbol{U})\|^2 + E_2^2(\boldsymbol{U})]^{1/2} \tag{22}$$

which appears as an extension of the objective (8) used for a plane analysis. The second term, E_2, is defined in such a way that $E_2 = 0$ when all specifications are met, and $E_2 > 0$ otherwise [51].

Once again, to solve the problem, F is minimized with respect to $\boldsymbol{U}$ by any nonlinear programming algorithm. However, this time the numerical procedure turns out to be very robust and reliable, and to be successfully applicable to both forced and autonomous circuits [53], [54]. The need for repeated nonlinear analyses is completely eliminated, and the gap between analysis and design CPU time requirements is effectively bridged. This partly happens because the number of unknown circuit parameters is usually small with respect to the number of harmonics in a well-posed problem, and partly because the availability of some degrees of freedom in the linear subnetwork often makes it easier for the minimization algorithm to reach the harmonic balance.

It is worth mentioning that the ability to carry out a constrained harmonic-balance analysis also allows some typical limitations of this class of techniques to be easily overcome. As an example, in an autonomous circuit the static solution of the circuit equations may be eliminated just by requiring a finite output power. Similarly, multiple operating points may be detected by adding suitable performance specifications [37], even if they do not belong to the same solution path from the viewpoint of continuation methods [35].

The high degree of maturity achieved by the technique described above leads to the easy prediction that any other conceptually related analysis algorithm may be successfully used in a quite similar way for optimization purposes. This is obvious, for instance, for the power-series method that was mentioned previously, since this is still a harmonic-balance approach, making use of a frequency-domain, rather than time-domain, device description. Another good candidate is what we called the "sample-balance" technique: in this case the unknowns to be simultaneously optimized would be represented by linear network parameters and time-domain samples of the state-variable waveforms.

Continuation methods have also been shown to be usable for nonlinear circuit optimization [32]–[34]. The underlying idea is still to avoid any full nonlinear analysis to be carried out within the minimization loop; however, this is now obtained by the typical philosophy of this kind of approach. The objective is optimized by a sequence of one-dimensional minimizations making use of a direct-search strategy such as Powell's method [29]. A regular analysis of the starting point is first performed by the standard stepped-parameter approach. In all subsequent objective-function evaluations the parameter is kept constant. Continuation is applied with respect to the circuit variables to generate the required steps of each one-dimensional search: the basic concept is essentially to keep small enough the steps along the search direction.

In this way every objective-function evaluation does require a nonlinear analysis, but this can be performed much more quickly than a regular one because a starting point very close to the solution is always available. The result is an order-of-magnitude speedup with respect to a brute-force optimization approach. However, the overall procedure is less efficient than the direct optimization described earlier, because the computation of the objective function is slower, and the one-dimensional search strategy is not optimal due to the limitations on step size.

An Example of Application

At this stage, we would like to discuss a simple example which is intended to give a feeling of what a powerful design tool a harmonic-balance optimization program may represent, and how deep an insight into circuit behavior can be obtained by this kind of technique. We consider the circuit depicted in Fig. 1 and we assume for the time being that the feedback branch AB is cut away so that we are simply left with a biased FET with input and output matching networks. It is quite clear that this topology can be used to do almost anything provided that the matching sections are suitably chosen. We assume that the circuit has to work as a regenerative frequency divider by two. For this purpose the input section is designed as a band-

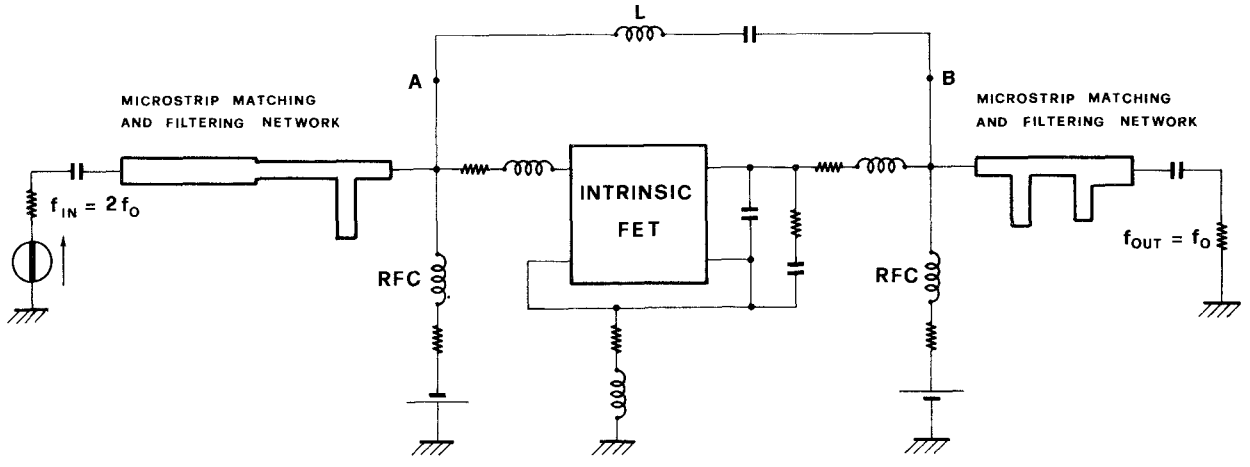

Fig. 1. Schematic topology of a microstrip regenerative frequency divider.

stop filter at the output frequency, and conversely, and the remaining degrees of freedom are optimized together with six gate and drain voltage harmonics for a conversion gain of 0 dB with an input power level of 6 mW at 9.4 GHz. What happens is that the optimization fails to converge, even though more complicated matching network topologies and different input drive levels are tried. An inspection of the results clearly shows the reason for this: the output frequency components cannot be balanced at the FET gate, because the device has an input impedance with a significant real part but is reactively loaded by the input filter. The two possible solutions are to suppress the input filter, which is obviously undesirable, or to introduce some degree of parallel feedback, such as connecting nodes A, B by an LC branch, as shown in Fig. 1. Once this has been done, the circuit can be designed with no further complications, and a behavior in agreement with experimental observations [55] can be predicted.

Of course, in this case the answer was *a priori* known, but the general principle still remains valid: even an unsuccessful optimization may provide useful design information, because the available circuit description is so detailed as to make it normally easy to find out where the difficulties come from. It is worth mentioning that the application of time-domain techniques to the same problem would only lead to the obvious result that the initial topology behaves as a low-efficiency frequency multiplier, with no indications on how the final goal could be met.

IV. Multiple-Frequency Excitation

The preceding discussion referred to nonlinear circuits supporting strictly time-periodic electrical regimes, described by a truncated Fourier expansion of the form (4). However, all results are equally valid for a quasi-periodic regime containing all possible intermodulation products of a number of non-harmonically related "exciting tones." In this case the mathematical representation (4) of the steady state is replaced by

$$x(t) = \sum_{\mathbf{k}} X_{\mathbf{k}} \exp\left(j \sum_{i} k_i \omega_i t \right) \tag{23}$$

($X^*_{-\mathbf{k}} = X_{\mathbf{k}}$), where ω_i is the angular frequency of the ith exciting tone. Truncation is now performed by taking into account only those intermodulation products whose order does not exceed a prescribed integer [56], that is,

$$\sum_{i} |k_i| \leqslant N_H. \tag{24}$$

It is worth mentioning that the term "exciting tone" should be interpreted here in the very broad sense of any sinusoidal signal existing in the circuit, independent of its physical origin. This includes sinusoidal pumps and autonomous oscillations, as well as any parametric or spurious tone that the circuit might generate.

With respect to the strictly periodic case, dealing with a quasi-periodic regime does not introduce any special conceptual difficulty; problems that do arise are essentially of a practical nature and invariably relate to numerical efficiency.

In the time domain, a direct integration can be performed in the usual way, independent of the number of sources acting in the circuit, until steady state is reached. However, in this case the steady state may have quite a long period—theoretically may not be periodic at all—which makes it difficult to determine how long it takes for the transient component to die out. Furthermore some typical multitone circuits, such as mixers with a low IF, may contain large time constants with respect to the RF period, which in turn may considerably slow down the achievement of steady-state conditions. Once again, some improvement may be obtained from shooting methods. For instance, Chua and Ushida [57] describe an algorithm based on a combination of shooting methods and least-squares waveform approximation, yielding both the initial point from which the network starts in steady state, and the Fourier coefficients of the steady state itself. However, the overall job still remains computationally heavy; frequency-domain methods are more appealing because of their ability to directly focus on the steady state.

From the standpoint of harmonic-balance techniques the critical step is the evaluation of the frequency-domain response of the nonlinear subnetwork to a quasi-periodic

input. In the case of commensurate frequencies, one could simply replace the quasi-periodic regime by a strictly periodic one by taking the greatest common divider of the exciting tones as the fundamental, and then proceed in the usual way [58]–[60]. Of course, if the fundamental is too low, the required sampling rate, and the corresponding size of the Fourier transforms, may turn out to be so large as to make this approach totally impractical. An efficient alternative is using a multidimensional grid of sampling points associated with multidimensional Fourier analysis to solve the problem [61]. This method has the advantage of being directly applicable to any combination of exciting frequencies, whether or not they be commensurate, with computational times independent of the actual frequency values. Another possible approach [62] is to carry out the transform by solving a linear system based on a nonuniform sampling scheme, whereby the sampling points are chosen so as to avoid ill-conditioning of the solving system.

These straightforward solution schemes are somewhat time-consuming, but have the advantage of programming simplicity, and provide a quasi-exact reference which can be used to establish the accuracy of approximate solutions.

As a matter of fact, a number of numerical procedures have been developed with the aim of reducing the computational burden of the harmonic-balance treatment of quasi-periodic regimes. For the sake of brevity we shall limit ourselves here to a short mention of some of the best-known and conceptually more relevant ones.

In [56] the response of the nonlinear subnetwork to a multitone excitation is uniformly sampled in the time domain. These samples are approximated in the least-squares sense by a generalized Fourier series of the form (23), thus producing an estimate of the spectral components of the nonlinear response.

In [63]–[65] the nonlinear subnetwork response is sampled at a much lower rate than the Nyquist rate, and Fourier transformed. To eliminate aliasing effects, the process is repeated a number of times with suitably shifted input spectra, and the resulting output spectra are linearly combined.

In [35] the original sparse spectrum (groups of lines separated by large gaps) is mapped onto an auxiliary dense spectrum (little or no gaps) by selecting a suitable set of conventional source frequencies. Calculations are carried out on the auxiliary spectrum, requiring a drastically reduced sampling rate.

In [66] each spectral component of interest is first shifted to dc by performing a frequency shift over the entire spectrum, and is then isolated by passing the shifted signal through a digital bandpass filter of suitable bandwidth.

Finally, a special mention is deserved by the power-series approach [67], [45], [68]. In this case the input and output spectral components are algebraically related by an explicit formula, which was developed by several authors in a number of subsequent steps [69]–[72], so that Fourier transforms are eliminated from the numerical procedure. Computational accuracy then only depends on the reliability of the power-series representation of the nonlinear subnetwork, and in particular on its convergence properties.

V. Frequency Conversion

An approximate solution has also been developed for the special case of a nonlinear circuit driven by two sinusoidal signals, one being very weak with respect to the other. This is commonly referred to as the mixer case, and is obviously very important from the technical viewpoint, which explains the good deal of attention that has been devoted to this specific subject. For once, there is almost general agreement in the technical literature as to how a mixer analysis problem should be dealt with. The commonly adopted approach relies upon the concept of the conversion matrix of the nonlinear subnetwork [73]–[80]. The basic idea is to consider the weaker, or radio-frequency (RF), signal as a small perturbation of a time-periodic steady-state regime, which may be established either by pumping the circuit with the stronger signal—the local oscillator (LO)—or by self-oscillation. The nonlinear subnetwork equations are then linearized in the neighborhood of the steady-state regime to find the circuit response to the injection of an additional small RF signal. Note the conceptual similarity of this approach to the conventional linearized description of the small-signal operation of a nonlinear device around a fixed bias point. As we shall see this analogy is of considerable help for an intuitive comprehension of a number of related topics, such as stability and noise.

In the mixer case, the periodic time dependence of the unperturbed regime leads to the generation of intermodulation products which in mixer terminology are called sidebands. Due to the assumed smallness of the RF signal, however, the situation is considerably simpler than for a general two-tone excitation, since only first-order products in ω_R may be retained. Let the steady-state regime established under LO drive with the RF signal suppressed be denoted by $\tilde{x}(t)$. Then the quasi-periodic regime under combined LO and RF excitation is represented to first order by

$$x(t) = \tilde{x}(t) + \mathrm{Re}\left[\sum_k \Delta X_k \exp\{j(\omega_R + k\omega_0)t\}\right] \quad (25)$$

where ω_0, ω_R are angular frequencies of the LO and RF signals, and ΔX_k is a vector of spectral components at the kth sideband. Similar expressions hold for the voltages and currents at the nonlinear subnetwork ports (with ΔX_k replaced by $\Delta V_k, \Delta I_k$, respectively).

If the nonlinear subnetwork equations (2) are now linearized around $\tilde{x}(t)$, linear relationships are established between the sideband amplitudes $\Delta X_k, \Delta V_k, \Delta I_k$. We can express such relationships by the compact matrix notation

$$\Delta V = P \Delta X$$
$$\Delta I = Q \Delta X \quad (26)$$

where ΔX is the vector of all ΔX_k's, and similar. We call (26) the *conversion equations* of the nonlinear subnetwork. In particular, if Q or P is nonsingular, we can eliminate

ΔX between eqs. (26) and write

$$\Delta V = PQ^{-1}\Delta I = Z_c\,\Delta I \tag{27}$$

or

$$\Delta I = QP^{-1}\Delta V = Y_c\,\Delta V \tag{28}$$

where Z_c, Y_c are the impedance conversion matrix and the admittance conversion matrix of the nonlinear subnetwork, respectively.

The time-domain description (2) of the nonlinear subnetwork lends itself nicely to a straightforward computation of the conversion matrices for a general nonlinear device [80]. In this case the Jacobians (11) must be available, since they are required to carry out the linearization. Making use of the expansion coefficients defined by (11), we introduce the square matrices of size n_D:

$$\begin{aligned} P_{k,p} &= \sum_{m=0}^{n} \{ j(\omega_R + k\omega_0) \}^m C_{m,p} \\ Q_{k,p} &= \sum_{m=0}^{n} \{ j(\omega_R + k\omega_0) \}^m D_{m,p} \end{aligned} \tag{29}$$

where n is defined in (2). Then the conversion matrices P, Q appearing in (26) are defined by [80]

$$\begin{aligned} P &\equiv [P_{k,s-k}] \\ Q &\equiv [Q_{k,s-k}] \end{aligned} \tag{30}$$

where s acts as the *row* index, and k as the *column* index, of the generic $(n_D \times n_D)$ submatrix. If N_H harmonics are retained to describe the local-oscillator regime, so that $-N_H \leqslant k \leqslant N_H$ as in (4), then the truncated size of the conversion matrices is given by the same number $N = n_D(2N_H + 1)$ defined by (7).

Note that the Fourier coefficients of the Jacobians used to compute (30) through (29) are the same ones needed to find the gradient of the harmonic-balance error through (12). Thus after performing a harmonic-balance analysis, such coefficients will automatically be available, and the derivation of the conversion matrix will become trivial. This is the reason why most mixer investigators use the harmonic-balance technique to determine the local-oscillator regime. For some simple devices these Fourier coefficients also have an immediate physical meaning: for instance, in the case of a nonlinear current source, they coincide with the Fourier coefficients of the differential conductance [73]. When (2) may be interpreted as the equations of a nonlinear equivalent circuit, it is also possible to combine the conversion matrices of elementary components by circuit-like algebra to find the conversion properties of the entire nonlinear subnetwork [77].

At this stage, mixer analysis has been reduced to a matter of linear circuit algebra. The situation is depicted in Fig. 2. The nonlinear subnetwork is replaced by a linear circuit described in the frequency domain by the conversion equations; each smaller block represents the linear subnetwork at one of the sidebands. Performing the required circuit connections leads to a matrix description of the mixer as the resulting two-port.

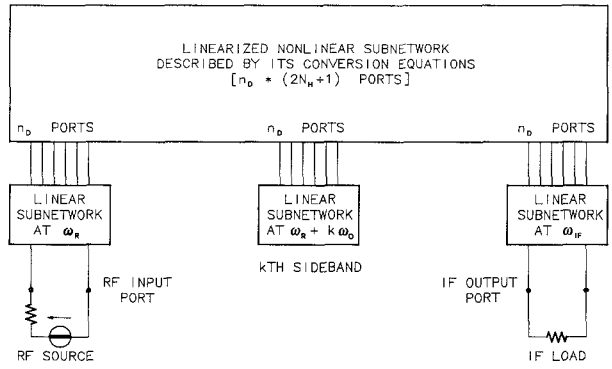

Fig. 2. Linearized equivalent circuit of a microwave mixer.

It is worth mentioning that this linearized behavior must be dealt with some caution. In fact, the two-port mixer matrix just mentioned is not usable for *design* purposes, except, of course, for a hand-driven optimization whereby a circuit parameter is manually changed and the whole analysis procedure is repeated each time. This is easily explained: assume, for instance, that an input matching network is designed on the basis of the linearized matrix description. If this network were connected with the RF port, the whole local oscillator regime would change, and so would the mixer matrix; the designed matching section would thus become meaningless. If we recall the analogy with the small-signal operation of a dc-biased nonlinear device, the same situation would occur if the addition of RF circuitry did result in a change of the bias point. The difference is that the bias circuit can be isolated from the RF by suitable dc-blocking devices, while obviously the local-oscillator regime cannot.

It follows that computer optimization of microwave mixers still remains an open problem: the only viable approach reported in the literature was a direct harmonic-balance optimization implemented on a supercomputer [59], [81].

It should be mentioned here that in the recent technical literature the mixer problem has been treated by several authors [58]–[60], [64], [82] as a conventional nonlinear analysis problem with multiple-frequency excitation (see Section IV). This approach is computationally heavier, but allows nonlinearizable aspects such as conversion-gain compression [59] and intermodulation distortion [82] to be accounted for. With some limitations, intermodulation distortion in diode mixers has also been analyzed by a stepwise procedure based on the conversion-matrix technique [83].

The frequency-conversion analysis outlined above is not only a numerical tool for the simulation and design of microwave mixers. It is also the kernel of a generalized perturbation analysis of periodic steady-state regimes supported by nonlinear microwave circuits. This analysis is compatible with a frequency-domain description of the linear subnetwork, and can thus take advantage of state-of-the-art techniques for passive circuit modeling [84], [85]. As will be shown in the following sections, such advanced and complicated problems as generalized stability and

noise analysis can be treated by the same perturbative approach with suitably chosen boundary conditions. Thus frequency-conversion analysis represents a key step toward the development of a general-purpose nonlinear microwave CAD system that is not confined to the traditional aspects of circuit simulation and optimization.

VI. Stability

If in Fig. 2 we suppress the RF source, the same circuit diagram becomes useful for investigating the stability of the local-oscillator regime. From a more general standpoint, the figure represents the linearized equivalent circuit of the original nonlinear network in the neighborhood of any time-periodic steady-state solution of the network equations. It may thus be used to establish a general-purpose approach to the stability analysis of any such solution which will be developed in the first part of this section. This analysis is restricted to *local* or *conditional* stability [86], in the sense that the results are only valid in the space of *small* perturbations of the steady state. Even if the latter is stable in this respect, a *large* perturbation may force the circuit to abandon it permanently and to jump to a different stable state. This wider viewpoint requires a *global* stability analysis, to be discussed in the second part of this section.

The stability analysis described here does not require any limiting or simplifying assumptions on circuit behavior and is thus considerably more advanced than most previously available solutions of the same problem [87]–[94], many of which it includes as particular cases. Its accuracy is only limited by the high-frequency behavior of the linear and nonlinear subnetwork models [94]. However, since this treatment is based on the same principles leading to mixer analysis via the conversion-matrix concept, its practical validity is indirectly but reliably checked by the large amount of successful mixer work available in the literature [73]–[79].

A. Local Stability

We first derive a characteristic equation for the natural frequencies of the linearized equivalent circuit shown in Fig. 2. Let a small perturbation of complex frequency $\sigma + j\omega$ be superimposed to the steady-state solution $\tilde{x}(t)$. The resulting electrical regime can be represented to first order by

$$x(t) = \tilde{x}(t) + \exp(\sigma t)\ \mathrm{Re}\left[\sum_k \Delta \boldsymbol{X}_k \exp\{j(\omega + k\omega_0)t\}\right] \tag{31}$$

which is identical to (25) except for the amplitude factor. Similar expressions hold for the voltages and currents. $\sigma + j\omega$ is a natural frequency of the steady state if the spectral components of the perturbation satisfy the linearized network equations. For the nonlinear subnetwork this means that (26) must hold with ω_R replaced by $\omega - j\sigma$. For the linear subnetwork, which is now source-free, we use the frequency-domain equations (3) with $\boldsymbol{D}(\omega) = 0$. We can gather all sidebands $\omega + k\omega_0$ into the compact matrix notation

$$\boldsymbol{A}_L \Delta \boldsymbol{V} + \boldsymbol{B}_L \Delta \boldsymbol{I} = 0 \tag{32}$$

where

$$\begin{aligned} \boldsymbol{A}_L &= \mathrm{diag}\left[\boldsymbol{A}(\omega - j\sigma + k\omega_0)\right] \\ \boldsymbol{B}_L &= \mathrm{diag}\left[\boldsymbol{B}(\omega - j\sigma + k\omega_0)\right]. \end{aligned} \tag{33}$$

Combining (26) with (33) yields the desired eigenvalue equation:

$$(\boldsymbol{A}_L \boldsymbol{P} + \boldsymbol{B}_L \boldsymbol{Q}) \Delta \boldsymbol{X} = 0 \tag{34}$$

so that the characteristic equation for the natural frequencies is

$$\det(\boldsymbol{A}_L \boldsymbol{P} + \boldsymbol{B}_L \boldsymbol{Q}) \equiv \Delta(\sigma + j\omega) = 0. \tag{35}$$

The above procedure can be considered the generalization of a result first discovered by Mees [95], [96]. The formulation adopted is convenient from the mathematical viewpoint, since the determinant (35) has no singularities except at infinity, so that pole–zero cancellations cannot occur. For the sake of physical intuition, however, it is better to rewrite (35) in terms of admittance or impedance matrices. Making use of (27) and (28) we get

$$\begin{aligned} \det(\boldsymbol{Z}_c + \boldsymbol{Z}_L) &= 0 \\ \det(\boldsymbol{Y}_c + \boldsymbol{Y}_L) &= 0 \end{aligned} \tag{36}$$

where

$$\begin{aligned} \boldsymbol{Z}_L &= \mathrm{diag}\left[\boldsymbol{Z}(\omega - j\sigma + k\omega_0)\right] \\ \boldsymbol{Y}_L &= \mathrm{diag}\left[\boldsymbol{Y}(\omega - j\sigma + k\omega_0)\right] \end{aligned} \tag{37}$$

and $\boldsymbol{Z}(\omega), \boldsymbol{Y}(\omega)$ are the conventional impedance and admittance matrix of the linear subnetwork. The eigenvalue equation is thus seen to be formally identical, and conceptually similar, to the one used to find the natural frequencies of a linear network. With respect to the latter case, the conventional device impedance or admittance matrix is replaced by the conversion matrix, while the single-frequency impedance or admittance of the linear subnetwork is replaced by the diagonal sum of all sideband impedances or admittances.

From the computational viewpoint it is virtually impossible to actually find all of the natural frequencies. Thus some indirect way of establishing the nature of the solutions has to be found. One possible approach is to produce a Nyquist stability plot [94]. In the present case, this turns out to be a much easier job than one might suspect, because of some known properties of the determinant. First of all, $\Delta(\sigma + j\omega)$ is a periodic function of ω, so that [94]

$$\Delta\left[\sigma + j(\omega + h\omega_0)\right] = (-1)^{nn_D h} \Delta(\sigma + j\omega) \tag{38}$$

where h is an integer. To remove the singularity of Δ at infinity ($\omega \to \infty$, $\sigma > 0$), we can thus replace Δ by the complex function, having the same finite zeros,

$$F_\Delta(\sigma + j\omega) = \exp\left[-\frac{nn_D \pi}{\omega_0}(\sigma + j\omega)\right] \Delta(\sigma + j\omega) \tag{39}$$

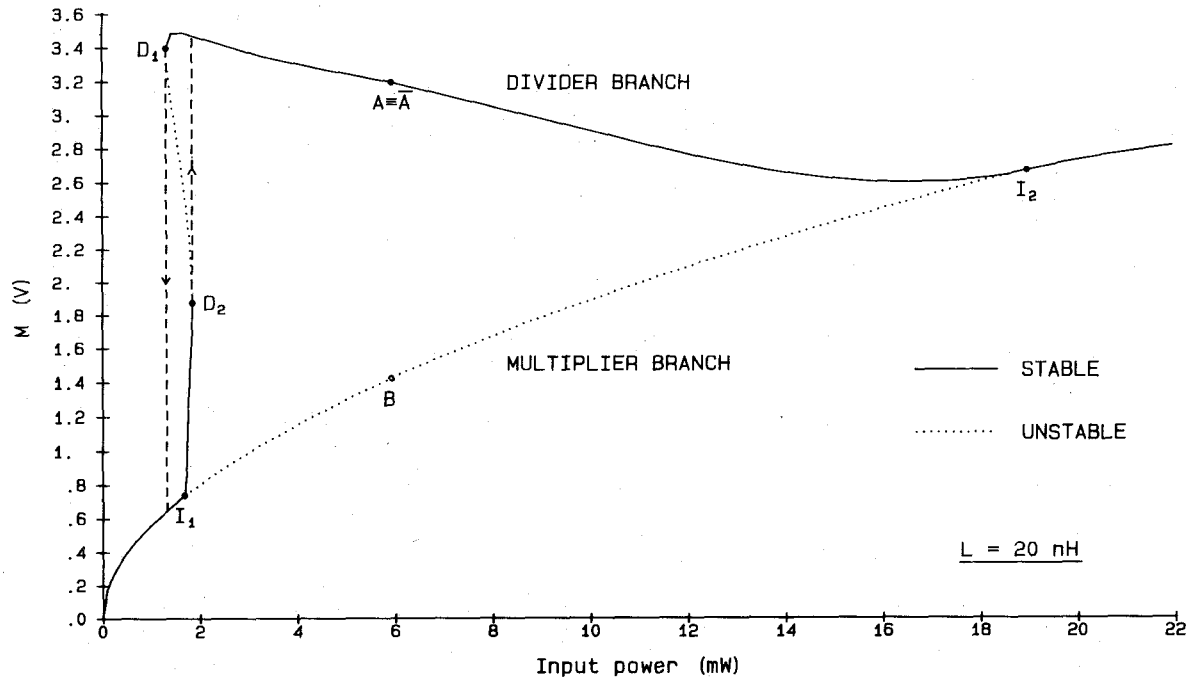

Fig. 3. Bifurcation diagram of the active frequency divider shown in Fig. 1.

which is periodic in ω with period ω_0. From Nyquist's equation [97], the number of natural frequencies lying in the region $[0 \leqslant \omega < \omega_0,\ \sigma > 0]$ is then given by the number of clockwise encirclements of the origin made by $F_\Delta(j\omega)$ as ω is swept from 0 to ω_0. It is assumed that the steady state considered is not a bifurcation point (see Section VI-B), so that $F_\Delta(j\omega) \neq 0$. Finally note that [94]

$$F_\Delta(\sigma - j\omega) = F_\Delta^*(\sigma + j\omega) \tag{40}$$

so that only the range $[0, \omega_0/2]$ need be investigated.

Of course in practice the user does not have to actually draw the Nyquist plot and count the encirclements: all this can be effectively done by the computer, and user interaction is reduced to a printed line on output reporting the total number of unstable natural frequencies. Furthermore, since the calculation is highly repetitive and easily vectorizable, it can be performed most efficiently on a supercomputer, typically in a fraction of a second in most practical cases. Thus it is actually possible to complement a general-purpose analysis and optimization program by an algorithm for local stability analysis in a way completely transparent to the user.

B. Global Stability

We first derive a global stability picture for a simple specific circuit by performing a large number of local stability analyses. Then we develop a systematic approach to global stability based on bifurcation theory, and show that in the particular case under examination the two sets of results strictly agree.

Let us consider once again the regenerative frequency divider introduced in Section III. Fig. 3 shows a bifurcation diagram for this circuit, which is drawn in terms of the quantity

$$M = \left(\sum_{k=1}^{N_H} \|\boldsymbol{X}_k\|^2 \right)^{1/2} \tag{41}$$

versus available input power. The state variables are chosen as the FET gate and drain voltages (Fig. 1).

To find this plot, the divider was first optimized for a 0-dB gain at an input power of 6 mW at 9.4 GHz, which yielded point A. This point is obviously associated with another steady state, which we name $\bar{A}$, having exactly the same harmonics except for a sign reversal of the odd ones. Finally, a third operating point, named B, was found at the same power level by a harmonic-balance analysis of the circuit with a zero starting point. The curves were then generated by a continuation method (e.g., [33], [35]), and the stability of a large number of points was checked by the Nyquist approach. The results of this analysis are reported in Fig. 3. Note that between points I_1 and I_2 three solution branches exist. Two of them are superimposed in the figure, and correspond to the usual bistable divider operation with a 180° phase shift between the two otherwise identical stable states. The third one is indicated as "multiplier branch" in the figure because of the total absence of any odd harmonics in the steady state. This can be expected to be unstable on a physical ground, since the pumped nonlinear device must produce a negative resistance, and thus unstable eigenvalues, for the onset of frequency division to take place.

This kind of analysis may be produced in a much more systematic way making use of the principles of bifurcation theory [86]. For a parameterized nonlinear system, bifurcations are defined as the states corresponding to those parameter values for which system stability undergoes an

abrupt qualitative change; that is, the real part of one (at least) natural frequency changes sign. For a circuit depending on a free parameter ρ, the existence of a bifurcation at $\rho = \rho_B$ requires that (5) and (35) be simultaneously satisfied with $\sigma = 0$, so that the mathematical conditions defining a bifurcation are

$$\boldsymbol{E}(\boldsymbol{X}, \rho_B) = 0$$
$$\Delta(j\omega, \boldsymbol{X}, \rho_B) = 0 \tag{42}$$
$$\frac{d\sigma}{d\rho}(\rho_B) \neq 0. \tag{43}$$

The topological as well as the stability-exchange properties of bifurcations in nonlinear systems have been studied very extensively under very broad assumptions which certainly warrant the application of the results to microwave circuits [86]. A simplified classification of the fundamental types of bifurcations (which are essentially the interesting ones for microwave applications) is given below [98].

The bifurcations of periodic solutions of period T_0 are considered first. We denote a periodic steady state by ${}_kS^m$, where k is the number of unstable natural frequencies and m indicates a period mT_0 (1 understood). Then the following fundamental types of bifurcations are possible [99]:

1) D-Type (Double-Point Bifurcation): A simple real natural frequency crosses the origin at $\rho = \rho_B$, so that equations (42) are satisfied with $\omega = 0$. The exchange of stability is defined by

$${}_kS + {}_{k\pm1}S \leftrightarrows {}_{k\pm1}S + {}_kS \tag{44}$$

where the states appearing first (second) on both sides of the arrows correspond to each other.

Special Case of D-Type (Regular Turning Point): This is the same as 1), but the creation or annihilation of two periodic states takes place at $\rho = \rho_B$. The exchange of stability is defined by

$$\phi \leftrightarrows {}_{k\pm1}S + {}_kS \tag{45}$$

where ϕ denotes the absence of solutions.

2) I-Type (Period-Doubling Bifurcation): Two simple complex-conjugate natural frequencies of the form $\sigma \pm j\omega_0/2$ cross the imaginary axis at $\rho = \rho_B$, so that (42) are satisfied with $\omega = \pm\,\omega_0/2$. The exchange of stability is defined by

$${}_kS \leftrightarrows {}_{k\pm1}S + 2\ {}_kS^2. \tag{46}$$

Note that $\sigma \pm j\omega_0/2$ is in fact *the same* solution of the characteristic equation (35) because of the periodicity of Δ. This explains the subscript $k \pm 1$ in the first term on the right-hand side of (46).

3) Hopf-Type (Spurious-Exciting Bifurcation): Two simple complex-conjugate natural frequencies cross the imaginary axis at $\rho = \rho_B$, so that (42) are satisfied with $0 < |\omega| < \omega_0/2$. The exchange of stability is defined by

$${}_kS \leftrightarrows {}_{k\pm2}S + {}_k(\text{CLOSED CURVE}) \tag{47}$$

where the closed curve represents a quasi-periodic regime which is stable for $k = 0$ and unstable otherwise.

Because of (40), $\Delta(0)$ and $\Delta(j\omega_0/2)$ are real quantities. This means that (42) is a system of $N+1$ real equations in $N+1$ real unknowns $\boldsymbol{X}$, ρ_B for D- and I-type bifurcations, and is a system of $N+2$ real equations in $N+2$ real unknowns $\boldsymbol{X}$, ρ_B, ω in the case of Hopf bifurcations (N given by (7)). Thus the system is always well conditioned from a mathematical viewpoint. This also explains why 1)–3) represent the *fundamental* bifurcations: the existence of such bifurcations is mathematically possible in generic situations. On the other hand, more complex kinds of bifurcations requiring additional constraints to be imposed on the same variables appearing in (42) (e.g., $\omega = \omega_0/4$ for a period-quadrupling bifurcation) will only exist under exceptional circumstances.

The condition (43) (often referred to as the condition for *strict* loss of stability) must be checked at any solution of (42) to ensure that the solution itself actually represents a bifurcation. It is virtually impossible to do this directly, because the computation of $d\sigma/d\rho$ requires a knowledge of the third-order partial derivatives of the circuit equations [86], [100]. Fortunately, the Nyquist analysis described in Section VI-A allows (43) to be checked by elementary methods. In fact, all we need do is to show that the Nyquist plot actually crosses the origin at $\rho = \rho_B$, i.e., lies on opposite sides of the origin at $\rho = \rho_B \pm \delta\rho$ ($\delta\rho \ll \rho_B$) in the neighborhood of $\pm\,\omega$. In particular, this implies that the real quantities $\Delta[0, \boldsymbol{X}(\rho), \rho]$ and $\Delta[j\omega_0/2, \boldsymbol{X}(\rho), \rho]$ change sign at $\rho = \rho_B$ in the cases of D- and I-type bifurcations, respectively.

The preceding argument also indicates the most convenient way of solving the system (42): its first equation is first solved for $\boldsymbol{X}(\rho)$ by a continuation method; then $\Delta(0) = 0$ and $\Delta(j\omega_0/2) = 0$ are solved in the one-dimensional manifold $\boldsymbol{X}(\rho)$, and $\Delta(j\omega) = 0$ is solved in the two-dimensional manifold $[\omega, \boldsymbol{X}(\rho)]$. The procedure is then repeated for the bifurcating branches. Since the stability of the circuit does not change, by definition, along a branch not containing bifurcations, a global stability picture for the circuit being considered is readily obtained in this way. Note that this implies that the stability of an *infinite* number of possible states becomes known by a *finite* number of operations.

We now go back to the regenerative frequency divider shown in Fig. 1 and apply the above considerations to this circuit. In the present case, the parameter is chosen as the available power of the pump, i.e., $\rho = P_{\text{IN}}(\text{mW})$. We are interested in the range $0 \leqslant \rho \leqslant 22$.

The "multiplier branch" (Fig. 3) is first determined by a continuation method starting from $\rho = 0$. A local stability analysis of the bias point chosen ($V_{gs0} = -1.9$ V, $V_{ds0} = 6$ V) reveals that the circuit is dc stable; thus the multiplier branch is stable in the neighborhood of the origin. Two solutions of the system (42) are found on the multiplier branch within the range of interest: two I-type bifurcations (points I_1, I_2) at $\rho = \rho_1 \cong 1.7$ and $\rho = \rho_2 \cong 18.8$, respectively. The two-parameter bifurcation analysis reported below (see Fig. 4) shows that I_1, I_2 belong to the same eigenvalue $\sigma \pm j\omega_0/2$. Thus the multiplier branch is

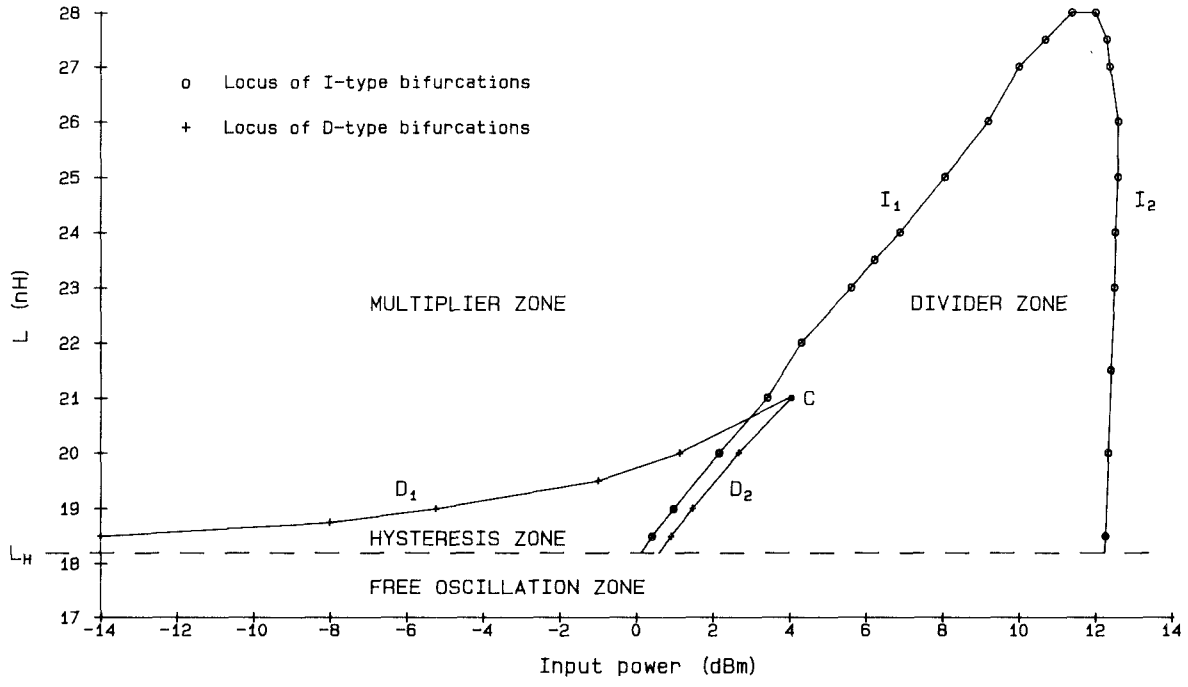

Fig. 4. Bifurcation analysis of the active frequency divider in a two- dimensional parameter space.

stable for $\rho < \rho_1$ and $\rho > \rho_2$ and unstable elsewhere. Starting at $\rho = \rho_1$, the "divider branch" is then determined by a continuation method. This branch starts at I_1 and terminates at I_2. The bifurcation at I_1 is *supercritical*, i.e., is described by (46) with the arrow pointing right and $k = 0$. Thus the divider branch is stable in the vicinity of the bifurcation. Two solutions of the system (42) are found on the divider branch within the range of interest: two D-type bifurcations corresponding to the regular turning points D_2, D_1 (Fig. 3). Because of (45), the divider branch becomes unstable beyond D_2. Once again, the two-dimensional bifurcation analysis reported below (Fig. 4) shows that D_1, D_2 belong to the same real eigenvalue. Thus the divider branch is stable beyond D_1, and a narrow hysteresis cycle appears around the threshold. Also, the nominal operating point A is found to be stable. Finally, frequency division ceases at point I_2, representing an I-type bifurcation of the *subcritical* kind (i.e., described by (46) with the arrow pointing left and $k = 0$). Note that each point of the divider branch is actually representative of two states, differing only in the sign of the odd harmonics, and thus associated with the same value of M.

A deeper insight into the global stability picture for the frequency divider is provided by a bifurcation analysis in a two-dimensional parameter space. The second parameter is chosen as the inductance L of the feedback branch, since feedback is expected to have a critical influence on circuit performance. The results are reported in Fig. 4.

On the L axis ($P_{IN} = 0$) a Hopf bifurcation of the bias point is encountered at $L = L_H \cong 18.2$ nH (Fig. 4). For $L \leqslant L_H$ the circuit behaves as a free-running oscillator with a fundamental around 4.7 GHz, and is thus useless as a frequency divider. In the region above L_H the circuit is dc-stable, and its qualitative behavior is always of the kind depicted in Fig. 3. The loci of the four relevant bifurcations I_1, I_2, D_1, D_2 are shown in the figure. The continuity of the two curves shows that I_1, I_2 are generated by the sign reversal of the real part of the same natural frequency, and so are D_1, D_2. Further note that the turning-point curve exhibits the classic pattern of the so-called "cusp catastrophe" [4], the cusp occurring at point C.

The overall behavior of the frequency divider is clearly apparent at a glance from Fig. 4. Frequency division will take place when the selected combination of inductance and drive power falls within the "divider zone." For any inductance value, the left-hand border of this region represents the divider threshold. A hysteresis cycle may exist around threshold, depending on the selected inductance value. Above the cusp point ($L \geqslant 21$ nH, approximately) hysteresis is eliminated, but threshold becomes relatively high (around 4 dBm). On the other hand, decreasing the inductance will lower the threshold, but at the same time a hysteresis cycle of growing width will appear. Furthermore, the circuit will become noisier, since the conditions for oscillation are approached.

As a final point, we shall briefly discuss the bifurcations of static solutions of the circuit equations ($X_k = 0$ for $k \neq 0$). In this case the fundamental bifurcations are the D- and the Hopf-type. For microwave applications, the latter plays an essential role in oscillator design and parasitic bias-circuit oscillations control in general microwave subsystems. The former may be of interest in relation to the design of dc-stable bias networks.

The conditions defining a bifurcation of a static solution are obviously much simpler than (42). If X_0 is the dc (and the only nonzero) component of the state vector at the

bifurcation, we must have

$$\boldsymbol{E}_0(\boldsymbol{X}_0, \rho_B) = 0$$

$$\det\left[\mathbf{1}_{n_D} - \boldsymbol{S}(\omega, \rho_B)\boldsymbol{S}_D(\omega, \boldsymbol{X}_0, \rho_B)\right] = 0 \tag{48}$$

$$\frac{d\sigma}{d\rho}(\rho_B) \neq 0 \tag{49}$$

where $\boldsymbol{S}$ is the conventional scattering matrix of the linear subnetwork (which may depend on the parameter ρ), and $\boldsymbol{S}_D$ is the small-signal scattering matrix of the nonlinear subnetwork describing its linearized behavior around the bias point defined by $\boldsymbol{X}_0$.

The exchange of stability at the bifurcation is discussed in detail in [98]. As a general rule, in the case of a simple real eigenvalue (D-type) or of two simple complex-conjugate eigenvalues (Hopf-type) crossing the imaginary axis at $\rho = \rho_B$, supercritical bifurcated states are stable, while subcritical ones are unstable [86].

For a D-type bifurcation ($\omega = 0$), (48) is a system of $n_D + 1$ real equations in $n_D + 1$ real unknowns $\boldsymbol{X}_0, \rho_B$. In the Hopf case, it is a system of $n_D + 2$ real equations in $n_D + 2$ real unknowns $\boldsymbol{X}_0, \rho_B, \omega$. Thus the system is generally solvable from the mathematical viewpoint. The solution is now simplified by the fact that the second of eqs. (48) simply states that one of the eigenvalues (in a conventional sense) of the matrix $\boldsymbol{S}\boldsymbol{S}_D$ must be equal to 1 at the bifurcation. Thus a convenient way of solving (48) is now as follows: i) the first of (48) is solved for $\boldsymbol{X}_0(\rho)$ by a continuation method; ii) to find D-type bifurcations, the one-dimensional manifold $\boldsymbol{X}_0(\rho)$ is searched for the points ρ_B at which one eigenvalue of $\boldsymbol{S}\boldsymbol{S}_D$ becomes unity; iii) to find Hopf-type bifurcations the two-dimensional manifold $[\omega, \boldsymbol{X}_0(\rho)]$ is searched for those points (ω, ρ_B) at which one eigenvalue of $\boldsymbol{S}\boldsymbol{S}_D$ becomes unity. To verify (49) we only have to check that the magnitude of the above-mentioned eigenvalue is <1 at $\rho_B - \delta\rho$ and >1 at $\rho_B + \delta\rho (\delta\rho \ll \rho_B)$, or conversely.

C. Stability Analysis in the Time Domain

In principle, a similar stability analysis can also be carried out by time-domain techniques.

Let us assume, for instance, that the circuit is described by the set of evolution equations (1). Static (dc) solutions may be obtained by setting $d\boldsymbol{x}_1/dt = d\boldsymbol{u}/dt = 0$ in (1) and then solving the resulting system of nonlinear algebraic equations. The original system is then linearized in the neighborhood of any dc solution to find the corresponding natural frequencies. The latter are given by the eigenvalues of the Jacobian of the right-hand side of (1) with respect to the state variables, evaluated in equilibrium conditions. Periodic steady-state solutions $\tilde{\boldsymbol{x}}(t)$ must first be determined by the techniques described in Section II-A. The system (1) is then linearized in the neighborhood of $\tilde{\boldsymbol{x}}(t)$ and the evolution of a small perturbation $\Delta\boldsymbol{x}(t)$ is studied by Floquet analysis [86]. This means that by further numerical integration one has to derive the *monodromy matrix* defining the change of the perturbation across one period T_0 of the steady-state:

$$\Delta\boldsymbol{x}(t + T_0) = \boldsymbol{\Phi}(T_0)\,\Delta\boldsymbol{x}(t). \tag{50}$$

The eigenvalues λ of $\boldsymbol{\Phi}(T_0)$ then yield the natural frequencies through the relationship

$$\lambda = \exp\{(\sigma + j\omega)T_0\}. \tag{51}$$

While the above procedure represents the conceptual basis for all mathematical treatments of stability, it is very difficult to implement numerically when the size of the system (1) is large (as is the case for practical microwave circuits), mainly because of the lengthy numerical integrations involved.

For this reason a true stability analysis is often replaced by a *transient* analysis [101], that is, a full numerical integration of the evolution equations from circuit turn-on up to the achievement of a steady state. It is implied that *all* natural frequencies will be excited during the transient, so that the effects of unstable ones will show up in the final waveforms. While this may be sufficient for many practical purposes, a global stability picture of the kind described in the preceding sections cannot be obtained in this way.

VII. Noise

In Section V we derived a generalized solution of the frequency-conversion (mixer) problem by injecting a small RF deterministic signal into a nonlinear network supporting a periodic steady-state regime, and by analyzing the resulting perturbation. When the RF source is replaced by a set of random noise generators as the perturbing mechanism, it is quite reasonable to expect that the same arguments will lead to a noise analysis of the steady state. Of course in this case the problem is much more complicated, since the free sources can only be described in a statistical sense. If several noise generators exist, they may not be statistically independent, and their correlation must be accounted for in evaluating the noise power delivered to a prescribed load. Further correlations are established among the noise sidebands because of the intermodulation of noise waveforms with the periodic steady state. All such effects are included in the general noise analysis to be presented in this section.

Because of its practical importance, a good deal of attention is paid to the noise problem in the technical literature. Several authors treat the subject for specific subsystems and with the aid of drastic simplifying assumptions, often aimed at the development of closed-form expressions highlighting some of its basic aspects [90], [92], [102]–[109]. Both frequency-domain [110], [111] and time-domain techniques [112] have been proposed to model the near-carrier noise in FET oscillators. Probably the most advanced treatment is given by Kerr in his noise analysis of diode mixers [74], [75], which makes use of a classic result established by Dragone [113] to correctly represent

the noise-sidebands correlation in the pumped diodes. The approach described here can be considered as an extension of Kerr's work to include generalized circuit topologies and multiport noisy nonlinear devices. As usual, the results are suitable for computer implementation in a general-purpose CAD environment.

Let us consider a stable steady-state solution $\tilde{x}(t)$ of the circuit equations, time-periodic of period $T_0 = 2\pi/\omega_0$, and let a random perturbation $\delta x(t)$ be superimposed on it. We assume that the perturbation is Fourier-transformable and write

$$\delta x(t) = \int_{-\infty}^{\infty} F_x(\omega) \exp(j\omega t)\, d\omega = \int_0^{\omega_0} \sum_k F_x(\omega + k\omega_0) \exp\{j(\omega + k\omega_0)t\}\, d\omega \quad (52)$$

where $F_x(\omega)$ is a vector of Fourier transforms (divided by 2π). All vectors appearing in (52) have the same size n_D, equal to the number of ports of the nonlinear (or linear) subnetwork.

In the following, our interest will mainly be focused on *spot* noise calculations, so that we shall consider noise perturbations of the form

$$\delta x(t) = \sum_k \delta X_k(\omega) \exp\{j(\omega + k\omega_0)t\} \qquad (0 < \omega < \omega_0) \quad (53)$$

where, according to (52)

$$\delta X_k(\omega) = F_x(\omega + k\omega_0)\, d\omega. \quad (54)$$

$\delta X_k(\omega)$ may be interpreted as a vector of complex amplitudes of "pseudosinusoidal" noise components at frequency $\omega + k\omega_0$ (i.e., at the kth sideband associated with ω). With the formulation adopted, the squared magnitude of the ith element of $\delta X_k(\omega)$ $(1 \leqslant i \leqslant n_D)$ represents the RMS value of those components of the noise waveform $\delta x_i(t)$ whose spectrum lies in a narrow band $d\omega$ in the neighborhood of $\omega + k\omega_0$. Thus if a spectral density $G_{xi}(\omega)$ can be associated with $\delta x_i(t)$, we have

$$|\delta X_{ki}(\omega)|^2 = G_{xi}(\omega + k\omega_0)\, d\omega. \quad (55)$$

To develop our noise analysis, we are going to replace the nonlinear network under consideration by the equivalent circuit shown in Fig. 5. This transformation requires some comments.

As usual, the original circuit is first subdivided into a linear and a nonlinear subnetwork. The vector of noise voltages at the connecting ports is denoted by $\delta v(t)$. The linear subnetwork is replaced by its Norton equivalent, consisting of a noise-free network with a noise current source connected across each port. These will be referred to as the "linear" noise sources and their set will be indicated by $j_L(t)$ (see Fig. 5). The linear noise sources are correlated, so that their statistical properties are described in terms of an $(n_D \times n_D)$ spot correlation matrix $\underline{\mathscr{C}}_L(\omega)$. If we adopt the representation (53), that is,

$$j_L(t) = \sum_k J_{Lk}(\omega) \exp\{j(\omega + k\omega_0)t\} \quad (56)$$

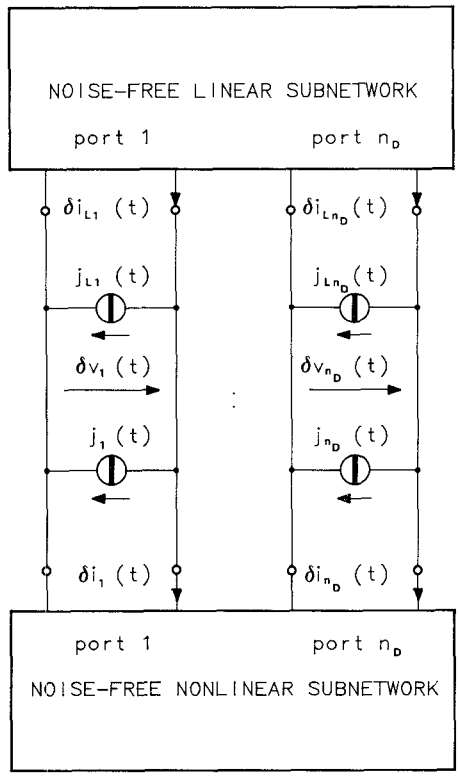

Fig. 5. Equivalent representation of a noisy nonlinear network.

then the correlation properties of the sidebands are expressed by

$$\langle J_{Lp}(\omega) J_{Lq}^*(\omega) \rangle = \delta_p^q \underline{\mathscr{C}}_L(\omega + p\omega_0) \quad (57)$$

where δ is Kronecker's symbol, $\langle\ \rangle$ indicates the statistical mean, and * the Hermitian conjugate. An important point is that a general computer algorithm, allowing $\underline{\mathscr{C}}_L(\omega)$ to be derived for a completely arbitrary configuration of the linear subnetwork, is available in the technical literature [114].

In Fig. 5 the noisy nonlinear subnetwork is dealt with in a similar way, i.e., is replaced by a noise-free nonlinear multiport with a noise current source connected across each port. Such sources account for the noise generated inside the nonlinear subnetwork and their properties are affected by the steady-state regime supported by the circuit, as described below. They will be referred to as the "nonlinear" noise sources, and their set will be denoted by $j(t)$ (see Fig. 5).

Note that the representation adopted for the nonlinear subnetwork does not have the meaning of a Norton equivalent circuit. In fact, the Norton transformation is based on the superposition principle, and its applicability is strictly confined to linear circuits. To produce the topology shown in Fig. 5, we simply open an additional external port of the nonlinear subnetwork at the terminals of each noise source which is not naturally connected across a port. For each fictitious port thus created, we must also add an open-circuited port to the linear subnetwork and a new state variable in the equations (2). Thus a noise analysis, although possible in general, may force us to

work with a number of ports n_D larger than required by a conventional nonlinear analysis not including noise.

We next derive the correlation properties of the nonlinear noise sources. Let us first focus our attention on the bias point of the nonlinear subnetwork, which is defined by the subset X_0 of the state vector X. If the nonlinear subnetwork were operated under dc conditions at the bias point X_0, its noise behavior would be described by a set of noise sources, namely $j_{dc}(X_0, t)$, depending on X_0 in a *deterministic* way. The statistical properties of j_{dc} can be derived in the usual way from the physical properties of the nonlinear subnetwork; for the most common microwave devices they are thoroughly described in the technical literature [115]. In particular, we will regard as known the spot correlation matrix of j_{dc}, namely $\underline{\mathscr{C}}_{dc}(X_0, \omega)$.

The dynamic case can now be studied by a quasi-static assumption. Following [113], we think of noise as arising from the superposition of statistically independent random disturbances whose duration is much smaller than T_0. The statistical properties are determined by the probability distribution of such elementary events, whose magnitude is proportional to a deterministic function of X_0. The periodic steady state may thus be treated as a time-dependent bias point: in this case the magnitude of the probability distribution is expressed by the same function with X_0 replaced by $\tilde{x}(t)$, and becomes a periodic function of time. We thus write

$$j(t) = h(t) j_{dc}(X_0, t) \tag{58}$$

where $h(t)$ is diagonal of size n_D, is time-periodic of period T_0, and has nonnegative elements. To evaluate $h(t)$, we consider the ith element of j_{dc} ($1 \leqslant i \leqslant n_D$), and denote by $G_{dci}(X_0, \omega)$ its spectral density. The corresponding (normalized) available noise power is given by

$$N_{dci} = \int_B G_{dci}(X_0, \omega)\, d\omega \tag{59}$$

where B is the noise bandwidth of interest. In the dynamic case, this power will be modulated by a periodic function of time, which can be identified as $h_i^2(t)$ according to (58). Using the quasi-static assumption we thus obtain from (59)

$$\begin{aligned} N_i(t) &= h_i^2(t) N_{dci} \\ &= \int_B G_{dci}\{\tilde{x}(t), \omega\}\, d\omega \end{aligned} \tag{60}$$

and finally

$$h_i(t) = \left[\frac{\int_B G_{dci}\{\tilde{x}(t), \omega\}\, d\omega}{\int_B G_{dci}(X_0, \omega)\, d\omega} \right]^{1/2} \qquad 1 \leqslant i \leqslant n_D. \tag{61}$$

Thus $h(t)$ can be immediately derived once the steady state $\tilde{x}(t)$ and the noise properties of the dc-biased nonlinear subnetwork are known.

Since $h(t)$ is real and time-periodic, we may write

$$h(t) = \sum_p H_p \exp(jp\omega_0 t) \tag{62}$$

where H_p is diagonal of size n_D, and $H_{-p} = H_p^*$.

Let us represent the static and dynamic noise current waveforms by expansions similar to (56) and denote by $J_{dck}(X_0, \omega)$ and $J_k(\omega)$ their pseudosinusoidal component amplitudes, respectively. Introducing such expansions and (62) into (58) yields

$$J_p(\omega) = \sum_k H_{p-k} J_{dck}(X_0, \omega). \tag{63}$$

Since the correlation properties of J_{dc} may be expressed as in (57) (with $\underline{\mathscr{C}}_L$ replaced by $\underline{\mathscr{C}}_{dc}$), from (63) we obtain directly

$$\langle J_p(\omega) J_q^*(\omega) \rangle = \sum_k H_{p-k} \underline{\mathscr{C}}_{dc}(X_0, \omega + k\omega_0) H_{k-q}. \tag{64}$$

Equation (64) shows that different sidebands of the nonlinear noise sources are in general correlated because of the modulation of the dc noise waveforms operated by the periodic steady state. It is easy to check that the result derived by Dragone [113] and used by Kerr [74], [75] can be reobtained from (64) in the case of a set of uncorrelated sources of white noise ($\underline{\mathscr{C}}_{dc}$ diagonal and independent of ω).

At this stage the noise analysis can be developed in a straightforward way. To make the equations formally simple, we first introduce for each noise waveform of interest the vector of the pseudosinusoidal component amplitudes at all sidebands: for instance, for the random perturbation $\delta x(t)$ we define

$$\delta X(\omega) \equiv [\delta X_k(\omega)] \tag{65}$$

and so forth. Such vectors satisfy a set of equations that are formally identical to (26) and (32), that is,

$$\begin{aligned} \delta V(\omega) &= P\, \delta X(\omega) \\ \delta I(\omega) &= Q\, \delta X(\omega) \\ A_L\, \delta V(\omega) &+ B_L\, \delta I_L(\omega) = 0 \end{aligned} \tag{66}$$

where the currents at the linear subnetwork ports have been denoted by the subscript L (see Fig. 5). From the figure we also obtain

$$\delta I_L(\omega) = \delta I(\omega) + J_L(\omega) + J(\omega). \tag{67}$$

Combining (66) and (67) yields

$$\delta V(\omega) = -P(A_L P + B_L Q)^{-1} B_L \{ J_L(\omega) + J(\omega) \}. \tag{68}$$

We can select the kth sideband by writing

$$\delta V_k(\omega) = U_k\, \delta V(\omega) \tag{69}$$

where

$$U_k \equiv [\cdots \mathbf{0} \cdots \mathbf{1}_{n_D} \cdots \mathbf{0} \cdots] \tag{70}$$

and $\mathbf{1}_{n_D}$ is an identity matrix of size n_D. Because of (35), the matrix $(A_L P + B_L Q)$ is nonsingular, and thus (68) is meaningful *at any* ω between 0 and ω_0, if the steady state

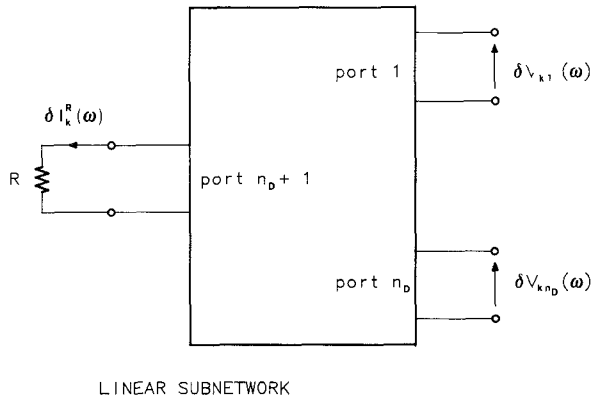

Fig. 6. Identification of a load within the linear subnetwork.

is asymptotically stable, i.e., all its natural frequencies have a negative real part.

To complete the noise analysis, we arbitrarily select a resistor within the linear subnetwork, which is assigned the meaning of load, and compute the spectral distribution of the noise power *actually delivered* to this load. For this purpose we rearrange the linear subnetwork in the way shown in Fig. 6, and carry out a conventional linear analysis of the (n_D+1)-port network thus obtained at $\omega + k\omega_0$. From the admittance matrix of the (n_D+1)-port, we can readily derive a $(1\times n_D)$ transadmittance matrix $\boldsymbol{Y}_R(\omega)$ such that

$$\delta I_k^R(\omega) = \boldsymbol{Y}_R(\omega + k\omega_0)\delta \boldsymbol{V}_k(\omega) \tag{71}$$

where $\delta I_k^R(\omega)$ is the complex amplitude of the pseudo-sinusoidal noise current component through R at $\omega + k\omega_0$. Making use of (69) and (68), we get

$$\delta I_k^R(\omega) = \boldsymbol{T}_k\{\boldsymbol{J}_L(\omega) + \boldsymbol{J}(\omega)\} \tag{72}$$

where

$$\boldsymbol{T}_k = -\boldsymbol{Y}_R(\omega + k\omega_0)\boldsymbol{U}_k\boldsymbol{P}(\boldsymbol{A}_L\boldsymbol{P} + \boldsymbol{B}_L\boldsymbol{Q})^{-1}\boldsymbol{B}_L. \tag{73}$$

Since the linear and nonlinear noise sources are not correlated, their effects may be superimposed in power. Thus the noise power delivered to R within a narrow frequency band $d\omega$ in the neighborhood of $\omega + k\omega_0$ is

$$\begin{aligned} dN_k(\omega) &= R\langle|\delta I_k^R(\omega)|^2\rangle \\ &= R\boldsymbol{T}_k\langle \boldsymbol{J}_L(\omega)\boldsymbol{J}_L^*(\omega)\rangle\boldsymbol{T}_k^* \\ &\quad + R\boldsymbol{T}_k\langle \boldsymbol{J}(\omega)\boldsymbol{J}^*(\omega)\rangle\boldsymbol{T}_k^*. \end{aligned} \tag{74}$$

If we now partition $\boldsymbol{T}_k$ into $(1\times n_D)$ submatrices, namely

$$\boldsymbol{T}_k \equiv [\boldsymbol{T}_{kp}] \tag{75}$$

and recall (57) and (64), we get the final result

$$\begin{aligned} dN_k(\omega) &= R\sum_p \boldsymbol{T}_{kp}\underline{\mathscr{C}}_L(\omega + p\omega_0)\boldsymbol{T}_{kp}^* \\ &\quad + R\sum_{p,q}\boldsymbol{T}_{kp}\Big\{\sum_s \boldsymbol{H}_{p-s}\underline{\mathscr{C}}_{DC}(\boldsymbol{X}_0, \omega + s\omega_0)\boldsymbol{H}_{s-q}\Big\}\boldsymbol{T}_{kq}^*. \end{aligned} \tag{76}$$

By means of (76), noise in a nonlinear network is essentially described as a frequency conversion effect, with each $\boldsymbol{T}_{kp}$ playing the role of a sideband-to-sideband conversion matrix. In particular, the quantity

$$\begin{aligned} dN_k^0(\omega) &= R\boldsymbol{T}_{k0}\underline{\mathscr{C}}_L(\omega)\boldsymbol{T}_{k0}^* \\ &\quad + R\sum_{p,q}\boldsymbol{T}_{kp}\boldsymbol{H}_p\underline{\mathscr{C}}_{\mathrm{dc}}(\boldsymbol{X}_0, \omega)\boldsymbol{H}_q^*\boldsymbol{T}_{kq}^* \end{aligned} \tag{77}$$

represents the contribution due to the up-conversion of baseband noise to the kth sideband. If the usual truncation is adopted, all summation indexes in (76) and (77) range from $-N_H$ to N_H.

Besides the noise power described by (76), having a continuous spectral distribution, a finite power is obviously delivered to the load at each harmonic of the steady state. This can be expressed as

$$S(k\omega_0) = \frac{1}{2}R|\boldsymbol{Y}_R(k\omega_0)\boldsymbol{\Phi}_k(\boldsymbol{X})|^2 \tag{78}$$

where $\boldsymbol{X}$ is the state vector, and $\boldsymbol{\Phi}_k$ is the kth harmonic of the first of (2) computed in steady-state conditions. Equation (78) represents a set of discrete spectral lines that are superimposed to the continuous spectrum (76).

VIII. Impact of Supercomputers

It has now become evident from the preceding discussion that nonlinear analysis and design problems concerning realistic microwave circuits may be large-size ones from the numerical standpoint. Many kinds of passive components require the use of sophisticated modeling techniques, while the nonlinear equivalent circuits of even the simplest microwave devices often contains several nonlinear elements such as resistors or dependent sources. Basic operations such as analysis and optimization require expensive search algorithms involving repeated multifrequency analyses of the linear subnetwork. The number of unknowns may be quite large, especially for broad-band operation, not to mention the case of multitone excitation such as in mixer or intermodulation problems. Stability and noise analyses require large-order matrices to be repeatedly evaluated and inverted. In order to implement all this, from the viewpoint of both software development and systematic use, it is rather natural to resort to the highest available computational power, namely, supercomputers.

For the time being, let us make use of a simple performance-oriented definition of a supercomputer, i.e., something that is roughly two orders of magnitude faster than a VAX and has several millions 64-bits words of central semiconductor memory. There are many reasons why such a machine can be attractive for nonlinear microwave CAD purposes, and some of them are conceptually more relevant than mere computational speedup. Of course, the latter is important by itself: some advanced nonlinear applications may require such a long CPU time as to make the use of a medium-size mainframe definitely impractical.

There is, however, much more than that. The computer-aided solution of any problem of applied science always

requires some amount of analytical preprocessing. There is always a tradeoff between mathematical and numerical work, and the use of sophisticated analytic and programming techniques is often convenient in order to alleviate the computational burden committed to the machine. On supercomputers, the opposite is often true: in fact, not only are they fast, but the simpler program architecture, the faster they perform, as we shall discuss later. Thus it may be convenient to waive a consistent part of the programmer's task and to rely upon the number-crunching capabilities of the computer. Simple, straightforward solution approaches which would be out of the question on medium-size scalar machines may now become the most natural way to solve the problem. An example concerning nonlinear microwave circuits under multiple-frequency excitation is reported in [59].

The availability of virtually unlimited memory resources is another important point. Once again, the classic tradeoff between memory occupation and computational speed may be pushed all the way in favour of numerical efficiency. To do the same on smaller-size machines one must often resort to virtual memory, which can slow down computation in a significant way.

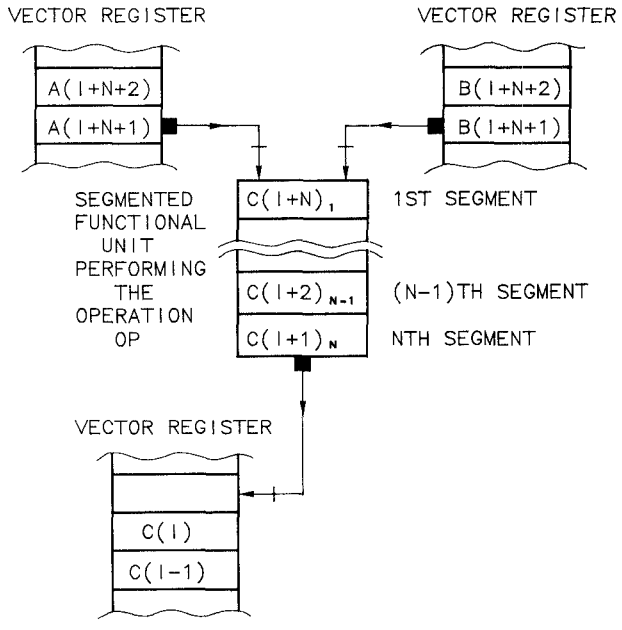

Fig. 7. Schematic illustration of the pipeline concept. $C(J)_k$ denotes the kth step of the computation of $A(J)$ OP $B(J)$ in the segmented functional unit.

A. Vector Processors

The increased computational power of supercomputers relies upon two fundamental mechanisms: technological advance and architectural evolution. The former is transparent to the user, and will not be considered here, but the latter is not, in the sense that codes should usually be matched to computer architecture in order to achieve maximum efficiency. In turn, architectural evolution with respect to the classic Von Neumann structure is essentially based on one of the fundamental concepts of modern computer science, namely, parallel processing.

As a matter of fact, most present-day supercomputers belong to the special class of vector processors [116], [117]. Vector processors are really available commercially and are relatively widespread; they feature the highest available computational power and are easily accessible to any user for general-purpose scientific calculations. In such machines, parallel processing is implemented by a number of basic mechanisms, the most important of which are listed below:

- pipelining of vector operations;
- chaining of vector operations;
- parallel execution of independent operations (arithmetic, logical, address calculations, $\cdots$) on independent functional units;
- parallel execution of vector and scalar operations;
- multitasking.

Pipelining is the fundamental aspect, and is schematically illustrated in Fig. 7 [118], [119]. Let us consider a binary operation of the form

$$C(I) = A(I) \text{ OP } B(I) \tag{79}$$

where OP is any arithmetic or logical operator and I is an integer index. This operation is actually executed through a number of elementary steps, each requiring one clock period, such as sign control, exponent fitting, addition of mantissas, and normalization, for a floating-point addition. The functional unit is thus subdivided into a corresponding number of cascaded subunits or segments, each performing one of the elementary steps.

Now assume that the code is carrying out a sequence of identical operations for increasing values of I, namely a vector operation, so that operands are continuously fed to the functional unit at a rate of a couple for each clock period. Once the entire process has been initialized, that is, after the vector startup time has elapsed, results will also be produced at the same rate. Thus the vector processor will execute binary vector operations at a peak speed, measured in floating-point operations per second, or flops, equal to the inverse of the clock period.

However, pipelining is not restricted to the binary case illustrated in Fig. 7: in fact, more complex vector operations can be executed in parallel in the pipeline sense (one result per clock period) by an additional mechanism, named chaining [117]. The concept is very simple: as soon as a result becomes available in a vector register (strictly speaking, one cycle later), it can be fed to the input of a different functional unit to serve as an operand for the subsequent operation. In this way the vector hardware may be configured as an extended functional unit with several inputs, where a multiple-operand arithmetic or logical operation can be pipelined.

All this is obviously handled by the compiler and is transparent to the user, except for one aspect: the calculations to be performed by the program should be organized into the largest possible groups of consecutive operations of the same kind, that is, into vector operations of the

maximum possible length. This is what we mean by *vectorizing* a program.

The other mechanisms mentioned above are in fact something different, in that they implement a more conventional concept of parallelism, namely, different functional units simultaneously execute independent operations on different operands. Multitasking is similar except that parallelism is exploited here at the highest level: if the system is a multiprocessor, the user's program can be organized into sections to be run concurrently on different CPU's. Organizing the tasks and synchronizing them when several ones merge again into a single instruction stream is up to the user, and can be done at the FORTRAN programming level by suitable calls to specialized system subroutines.

Note that the above discussion is somewhat Cray-oriented since this is the system family the authors are most familiar with; however, the principles are substantially valid for many different kinds of vector processors.

The same discussion makes it clear that program vectorization is the most important action to be taken in order to effectively exploit the computational power of a vector supercomputer. The same code on the same machine can run in a CPU time ranging from, say, 1 to 10 in relative terms depending on its degree of vectorization. This has a direct impact on computer costs, too: in fact, the user will pay exactly the same amount for one CPU second regardless of whether his calculations are vectorized or fully scalar. This means that any speedup obtained by vectorization will result in a cost reduction by exactly the same amount. An important related point is that vectorizing invariably means making a program simpler and better structured, which is clearly shown by the fact that vectorized programs are usually more efficient from the scalar viewpoint, too [122], [123]. This happens because vectorizing leads to the elimination of a number of nonproductive but time-consuming procedures such as *if* statements and subroutine calls. Of course this does not imply that vectorization is good for scalar machines, since it always results in a large increase of memory requirements. In fact, space has to be provided to store the entire vector operands, which must be physically available, while in the scalar approach subsequent elements may overwrite the same memory locations, since results are produced sequentially rather than in parallel.

B. Supercomputers in Microwave CAD

Going back to our main subject, it is quite obvious that a nonlinear microwave CAD program is a natural candidate for an efficient vectorization. For instance, a circuit optimization is usually carried out by some sort of iterative method, and is thus a highly repetitive job, which will spend most of the CPU time in executing exactly the same set of operations over and over again. Thus in principle vectorizing just becomes matter of organizing such operations in a convenient order.

Let us focus our attention on a relatively expensive numerical procedure such as the optimization of a nonlinear circuit by the harmonic-balance approach. Three mechanisms are essentially responsible for the computer time requirement of this kind of job, namely, sampling the time-domain response of the nonlinear subnetwork, Fourier transforming it, and analyzing the linear subnetwork at all the design frequencies and their harmonics. The relative importance of these aspects is strongly job-dependent; however, they are usually responsible for more than 90 percent of the overall time, so this is where the vectorization effort has to be spent.

TABLE II
PERFORMANCE OF A TYPICAL VECTOR PROCESSOR (CRAY X-MP)

1) FFT (N_s = NUMBER OF SAMPLING POINTS)		
	$N_s = 32$	$N_s = 1024$
VECTOR SPEEDUP	7.3	14.7
COMBINED SPEEDUP WITH RESPECT TO THE CDC 7600	19 3	39 0
2) SAMPLING OF NONLINEAR RESPONSE		
	$N_s = 32$	$N_s = 1024$
VECTOR SPEEDUP	6.5	11.9
COMBINED SPEEDUP WITH RESPECT TO THE CDC 7600	18.9	34.7
3) MULTIFREQUENCY LINEAR SUBNETWORK ANALYSIS (N_F = NUMBER OF FREQUENCIES)		
	$N_F = 7$	$N_F = 49$
VECTOR SPEEDUP	2.9	5.9
COMBINED SPEEDUP WITH RESPECT TO THE CDC 7600	14 6	29.7

Typical speedups measured on a Cray X-MP system are reported in Table II. Of course the FFT represents the easiest and most rewarding job since fully vectorized and very efficient subroutines performing this algorithm are available in all supercomputer libraries.

As for the nonlinear response, vectorization here is up to the user, but is still easy and may be carried out by direct application of elementary principles. The scalar approach would be to code the nonlinear subnetwork equations in a subroutine yielding the response at a given time, and then to repeatedly call it at all sampling instants. In a vector logic one has to move the iteration inside the subroutine, so that the calculation of the entire response becomes a unique vector operation; in other words all sampling points are processed in parallel in the pipeline sense.

The approach to the linear subnetwork analysis is conceptually similar: a sequence of single-frequency analyses is changed into a single multifrequency analysis; that is, any aspect of network performance is treated simultaneously at all frequencies of interest. In this case, to enhance the degree of vectorization and thus to improve the overall performance, some further actions can be taken, such as the parallel computation of all physically similar circuit components, and the parallel execution of topologically similar component connections. These ideas have been discussed in detail in the recent technical literature [123].

The results shown in Table II include a comparison with the performance of an equivalent scalar code on a classic scalar mainframe such as the Cyber 76. Very similar results are obtained with modern scalar systems such as the VAX 8800. The figures clearly show that supercomputers can indeed be used to carry out large applications with fast job turnaround and good cost-to-performance ratio and have the potential to bridge the gap between linear and nonlinear microwave CAD techniques.

REFERENCES

[1] "Nonlinear analysis and design of microwave circuits", in *Proc. 15th European Microwave Conf.*, Tutorial Session no. 2 (Paris), Sept. 1985, pp. 1087–1124.

[2] C. A. Desoer, Ed., Special Issue on Nonlinear Circuits, *IEEE Trans. Circuit Theory*, vol. CT-19, Nov. 1972.

[3] R. W. Lin, Ed., Special Issue on Nonlinear Circuits and Systems, *IEEE Trans. Circuits Syst.*, vol. CAS-27, Nov. 1980.

[4] L. O. Chua, Ed., Special Issue on Nonlinear Phenomena, Modeling, and Mathematics, *IEEE Trans. Circuits Syst.* vol. CAS-30, Aug.–Sept. 1983.

[5] E. S. Kuh, Ed., Centennial Issue, *IEEE Trans. Circuits Syst.*, vol. CAS-31, Jan. 1984.

[6] D. O. Pederson, "A historical review of circuit simulation," *IEEE Trans. Circuits Syst.*, vol. CAS-31, pp. 103–111, Jan. 1984.

[7] V. K. Tripathi and J. B. Rettig, "A SPICE model for multiple coupled microstrips and other transmission lines," in *1985 IEEE MTT-S Int. Microwave Symp. Dig.* (St. Louis), Sept. 1985, pp. 703–706.

[8] J. E. Schutt-Aine and R. Mittra, "Analysis of pulse propagation in coupled transmission lines," *IEEE Trans. Circuits Syst.*, vol. CAS-32, pp. 1214–1219, Dec. 1985.

[9] F. Romeo and M. Santomauro, "Time-domain simulation of *n*-coupled transmission lines," *IEEE Trans. Microwave Theory Tech.*, vol. MTT-35, pp. 131–137, Feb. 1987.

[10] S. E. Sussman-Fort, S. Narasimhan, and K. Mayaram, "A complete GaAs MESFET computer model for SPICE," *IEEE Trans. Microwave Theory Tech.*, vol. MTT-32, pp. 471–473, Apr. 1984.

[11] A. K. Jastrzebski and M. I. Sobhy, "Analysis of microwave circuits using state-space approach," in *Proc. 1984 IEEE Int. Symp. Circuits Syst.* (Montreal), May 1984, pp. 1119–1122.

[12] J. M. Golio, P. A. Blakey, and R. O. Grondin, "A general CAD tool for large-signal GaAs MESFET circuit design," in *1985 IEEE MTT-S Int. Microwave Symp. Dig.* (St. Louis), June 1985, pp. 417–420.

[13] M. I. Sobhy and A. K. Jastrzebski, "Direct integration methods of non-linear microwave circuits," in *Proc. 15th European Microwave Conf.* (Paris), Sept. 1985, pp. 1110–1118.

[14] C. W. Gear, "Simultaneous numerical solution of differential-algebraic equations," *IEEE Trans. Circuit Theory*, vol. CT-18, pp. 89–95, Jan. 1971.

[15] P. M. Russo, "On the time-domain analysis of linear time-invariant networks with large time-constant spreads by digital computers," *IEEE Trans. Circuit Theory*, vol. CT-18, pp. 194–197, Jan. 1971.

[16] R. L. Veghte and C. A. Balanis, "Dispersion of transient signals in microstrip transmission lines," *IEEE Trans. Microwave Theory Tech.*, vol. MTT-34, pp. 1427–1436, Dec. 1986.

[17] J. F. Whitaker *et al.*, "Pulse dispersion and shaping in microstrip lines," *IEEE Trans. Microwave Theory Tech.*, vol. MTT-35, pp. 41–47, Jan. 1987.

[18] L. W. Nagel, "SPICE2: A computer program to simulate semiconductor circuits," Electronic Research Laboratory, University of California-Berkeley, Memo ERL-M520, 1975.

[19] T. Brazil *et al.*, "Large-signal FET simulation using time domain and harmonic-balance methods," *Proc. Inst. Elec. Eng.*, pt. H, vol. 133, pp. 363–367, Oct. 1986.

[20] S. W. Director, "A method for quick determination of the periodic steady-state in nonlinear networks," in *Proc. 9th Allerton Conf. Circuit Syst. Theory*, (University of Illinois, Urbana-Champaign), Oct. 1971, pp. 131–139.

[21] T. J. Aprille Jr. and T. N. Trick, "Steady-state analysis of nonlinear circuits with periodic inputs," *Proc. IEEE*, vol. 60, pp. 108–114, Jan. 1972.

[22] T. J. Aprille Jr. and T. N. Trick, "A computer algorithm to determine the steady-state response of nonlinear oscillators," *IEEE Trans. Circuit Theory*, vol. CT-19, pp. 354–360, July 1972.

[23] F. R. Colon and T. N. Trick, "Fast periodic steady-state analysis for large-signal electronic circuits," *IEEE J. Solid-State Circuits*, vol. SC-8, pp. 260–269, Aug. 1973.

[24] S. Skelboe, "Computation of the periodic steady-state response of nonlinear networks by extrapolation methods," *IEEE Trans. Circuits Syst.*, vol. CAS-27, pp. 161–175, Mar. 1980.

[25] M. S. Nakhla and J. Vlach, "A piecewise harmonic-balance technique for determination of periodic response of nonlinear systems," *IEEE Trans. Circuits Syst.*, vol. CAS-23, pp. 85–91, Feb. 1976.

[26] J. C. Lindenlaub, "An approach for finding the sinusoidal steady state response of nonlinear systems," in *Proc. 7th Allerton Conf. Circuit Syst. Theory* (University of Illinois, Chicago), 1969.

[27] K. S. Kundert and A. Sangiovanni-Vincentelli, "Simulation of nonlinear circuits in the frequency domain," *IEEE Trans. Computer-Aided Design*, vol. CAD-5, pp. 521–535, Oct. 1986.

[28] D. M. Himmelblau, *Applied Nonlinear Programming.* New York: McGraw-Hill, 1972.

[29] M. J. D. Powell, "Minimization of functions of several variables," in *Numerical Analysis: An Introduction*, J. Walsh, Ed., Washington, D.C.: Thompson, 1967.

[30] R. Fletcher, "A new approach to variable metric algorithms," *Computer J.*, vol. 13, pp. 317–322, Aug. 1970.

[31] H. Wacker, *Continuation Methods.* New York: Academic Press, 1978.

[32] F. Filicori, V. A. Monaco, and C. Naldi, "Analysis and optimization of non-linear circuits with periodic excitation," in *Proc. SPACECAD '79* (Bologna), Sept. 1979, pp. 171–176.

[33] F. Filicori, V. A. Monaco, and C. Naldi, "Simulation and design of microwave Class-C amplifiers through harmonic analysis," *IEEE Trans. Microwave Theory Tech.*, vol. MTT-27, pp. 1043–1051, Dec. 1979.

[34] C. Naldi and F. Filicori, "Computer-aided design of GaAs MESFET power amplifiers," in *Proc. 12th European Microwave Conf.* (Helsinki), Sept. 1982, pp. 435–440.

[35] D. Hente and R. H. Jansen, "Frequency-domain continuation method for the analysis and stability investigation of nonlinear microwave circuits," *Proc. Inst. Elec. Eng.*, pt. H, vol. 133, pp. 351–362, Oct. 1986.

[36] L. O. Chua and A. Ushida, "A switching-parameter algorithm for finding multiple solutions of nonlinear resistive circuits," *Int. J. Circuit Theory Appl.*, vol. 4, pp. 215–239, 1976.

[37] V. Rizzoli *et al.*, "User-oriented software package for the analysis and optimization of nonlinear microwave circuits," *Proc. Inst. Elec. Eng.*, pt. H, vol. 133, pp. 385–391, Oct. 1986.

[38] F. B. Hildebrand, *Introduction to Numerical Analysis.* New York: McGraw-Hill, 1967.

[39] A. R. Kerr, "A technique for determining the local oscillator waveforms in a microwave mixer," *IEEE Trans. Microwave Theory Tech.*, vol. MTT-23, pp. 828–831, Oct. 1975.

[40] R. G. Hicks and P. J. Khan, "Numerical technique for determining pumped nonlinear device waveforms," *Electron. Lett.*, vol. 16, pp. 375–376, May 1980.

[41] R. G. Hicks and P. J. Khan, "Numerical analysis of nonlinear solid-state device excitation in microwave circuits," *IEEE Trans. Microwave Theory Tech.*, vol. MTT-30, pp. 251–259, Mar. 1982.

[42] C. Camacho-Peñalosa, "Numerical steady-state analysis of nonlinear microwave circuits with periodic excitation," *IEEE Trans. Microwave Theory Tech.*, vol. MTT-31, pp. 724–730, Sept. 1983.

[43] F. Filicori and C. Naldi, "An algorithm for the periodic or quasi-periodic steady-state analysis of non-linear circuits," in *Proc. 1983 IEEE Int. Symp. Circuits Syst.* (Newport Beach), May 1983, pp. 366–369.

[44] D. Hwang and T. Itoh, "Large-signal modeling and analysis of GaAs MESFET," in *Proc. 16th European Microwave Conf.* (Dublin), Sept. 1986, pp. 189–194.

[45] G. W. Rhyne and M. B. Steer, "A new frequency-domain approach to the analysis of nonlinear microwave circuits," in *1985 IEEE MTT-S Int. Microwave Symp. Dig.* (St. Louis), June 1985, pp. 401–404.

[46] G. L. Heiter, "Characterization of nonlinearities in microwave devices and systems," *IEEE Trans. Microwave Theory Tech.*, vol. MTT-21, pp. 797–805, Dec. 1973.

[47] R. S. Tucker, "Third-order intermodulation distortion and gain compression of GaAs FET's," *IEEE Trans. Microwave Theory Tech.*, vol. MTT-27, pp. 400–408, May 1979.

[48] F. Filicori, C. Naldi, and M. R. Scalas, "Non-linear circuit analysis through periodic spline approximation," *Electron. Lett.*, vol. 15, pp. 597–599, Sept. 1979.

[49] F. Filicori, M. R. Scalas,and C. Naldi, "Periodic steady-state analysis of non-linear circuits using spline functions," in *Proc. SPACECAD '79* (Bologna), Sept. 1979, pp. 189–193.

[50] S. W. Director and K. Wayne Current, "Optimization of forced nonlinear periodic circuits," *IEEE Trans. Circuits Syst.*, vol. CAS-23, pp. 329–335, June 1976.

[51] A. Lipparini, E. Marazzi, and V. Rizzoli, "A new approach to the computer-aided design of nonlinear networks and its application to microwave parametric frequency dividers," *IEEE Trans. Microwave Theory Tech.*, vol. MTT-30, pp. 1050–1058, July 1982.

[52] V. Rizzoli, A. Lipparini, and E. Marazzi, "A general-purpose program for nonlinear microwave circuit design," *IEEE Trans. Microwave Theory Tech.*, vol. MTT-31, pp. 762–770, Sept. 1983.

[53] A. Lipparini, E. Marazzi, and V. Rizzoli, "Computer-aided design of microwave parametric frequency dividers," in *1981 IEEE MTT-S Int. Microwave Symp. Dig.* (Los Angeles), June 1981, pp. 229–231.

[54] V. Rizzoli and A. Lipparini, "A computer-aided approach to the nonlinear design of microwave transistor oscillators," in *1982 IEEE MTT-S Int. Microwave Symp. Dig.* (Dallas), June 1982, pp. 453–455.

[55] C. Rauscher, "Regenerative frequency division with a GaAs FET," *IEEE Trans. Microwave Theory Tech.*, vol. MTT-32, pp. 1461–1468, Nov. 1984.

[56] A. Ushida and L. O. Chua, "Frequency-domain analysis of nonlinear circuits driven by multi-tone signals," *IEEE Trans. Circuits Syst.*, vol. CAS-31, pp. 766–779, Sept. 1984.

[57] L. O. Chua and A. Ushida, "Algorithms for computing almost-periodic steady-state response of nonlinear systems to multiple input frequencies," *IEEE Trans. Circuits Syst.*, vol. CAS-28, pp. 953–971, Oct. 1981.

[58] M. A. Smith *et al.*, "RF nonlinear device characterization yields improved modeling accuracy," in *1986 IEEE MTT-S Int. Microwave Symp. Dig.* (Baltimore), June 1986, pp. 381–384.

[59] V. Rizzoli, C. Cecchetti, and A. Neri, "Supercomputer-aided generalized mixer analysis and optimization," in *Proc. 16th Eurpoean Microwave Conf.* (Dublin), Sept. 1986, pp. 692–697.

[60] W. R. Curtice, "Nonlinear analysis of GaAs MESFET amplifiers, mixers, and distributed amplifiers using the harmonic balance technique," *IEEE Trans. Microwave Theory Tech.*, vol. MTT-35, pp. 441–447, Apr. 1987.

[61] V. Rizzoli, C. Cecchetti, and A. Lipparini, "A general-purpose program for the analysis of nonlinear microwave circuits under multitone excitation by multidimensional Fourier transform," in *Proc. 17th European Microwave Conf.* (Rome), Sept. 1987, pp. 635–640.

[62] G. B. Sorkin, K. S. Kundert, and A. Sangiovanni-Vincentelli, "An almost-periodic Fourier transform for use with harmonic balance," in *1987 IEEE MTT-S Int. Microwave Symp. Dig.* (Las Vegas), June 1987, pp. 717–720.

[63] R. J. Gilmore and F. J. Rosenbaum, "Modeling of nonlinear distortion in GaAs MESFETS," in *1984 IEEE MTT-S Int. Microwave Symp. Dig.* (San Francisco), June 1984, pp. 430–431.

[64] J. Dreifuss, A. Madjar, and A. Bar-Lev, "A full large-signal analysis of active microwave mixers," in *Proc. 16th European Microwave Conf.* (Dublin), Sept. 1986, pp. 687–691.

[65] R. Gilmore, "Nonlinear circuit design using the modified harmonic-balance algorithm," *IEEE Trans. Microwave Theory Tech.*, vol. MTT-34, pp. 1294–1307, Dec. 1986.

[66] M. Gayral *et al.*, "The spectral balance: A general method for analysis of nonlinear microwave circuits driven by non-harmonically related generators," in *1987 IEEE MTT-S Int. Microwave Symp. Dig.* (Las Vegas), June 1987, pp. 119–121.

[67] J. J. Bussgang, L. Ehrman, and J. W. Graham, "Analysis of nonlinear systems with multiple inputs," *Proc. IEEE*, vol. 62, pp. 1088–1119, Aug. 1974.

[68] G. W. Rhyne and M. B. Steer, "Simulation of intermodulation distortion in MESFET circuits with arbitrary frequency separation of tones," in *1986 IEEE MTT-S Int. Microwave Symp. Dig.* (Baltimore), June 1986, pp. 547–550.

[69] R. G. Sea, "An algebraic formula for amplitudes of intermodulation products involving an arbitrary number of frequencies," *Proc. IEEE*, vol. 56, pp. 1388–1389, Aug. 1968.

[70] R. G. Sea and A. G. Vacroux, "On the computation of intermodulation products for a power series nonlinearity," *Proc. IEEE*, vol. 57, pp. 337–338, Mar. 1969.

[71] G. B. Price and P. J. Khan, "Large-signal analysis of semiconductor circuits with multifrequency excitation," *Proc. IEEE*, vol. 67, pp. 177–178, Jan. 1979.

[72] M. B. Steer and P. J. Khan, "An algebraic formula for the output of a system with large-signal, multifrequency excitation," *Proc. IEEE*, vol. 71, pp. 177–179, Jan. 1983.

[73] S. Egami, "Nonlinear, linear analysis and computer-aided design of resistive mixers," *IEEE Trans. Microwave Theory Tech.*, vol. MTT-22, pp. 270–275, Mar. 1974.

[74] D. N. Held and A. R. Kerr, "Conversion loss and noise of microwave and millimeter-wave mixers: Part 1—Theory," *IEEE Trans. Microwave Theory Tech.*, vol. MTT-26, pp. 49–55, Feb. 1978.

[75] A. R. Kerr, "Noise and loss in balanced and subharmonically pumped mixers: Part 1—Theory," *IEEE Trans. Microwave Theory Tech.*, vol. MTT-27, pp. 938–943, Dec. 1979.

[76] M. T. Faber and W. K. Gwarek, "Nonlinear–linear analysis of microwave mixers with any number of diodes," *IEEE Trans. Microwave Theory Tech.*, vol. MTT-28, pp. 1174–1181, Nov. 1980.

[77] S. A. Maas, "Theory and analysis and GaAs MESFET mixers," *IEEE Trans. Microwave Theory Tech.*, vol. MTT-32, pp. 1402–1406, Oct. 1984.

[78] J. Dreifuss, A. Madjar, and A. Bar-Lev, "A novel method for the analysis of microwave two-port active mixers," *IEEE Trans. Microwave Theory Tech.*, vol. MTT-33, pp. 1241–1244, Nov. 1985.

[79] J. Dreifuss *et al.*, "Application of the harmonic-balance method to analysis of MESFET oscillators and dual-gate MESFET mixers," in *Proc. 15th European Microwave Conf.* (Paris), Sept. 1985, pp. 521–526.

[80] V. Rizzoli, C. Cecchetti, and A. Lipparini, "Frequency conversion in general nonlinear multiport devices," in *1986 IEEE MTT-S Int. Microwave Symp. Dig.* (Baltimore), June 1986, pp. 483–486.

[81] V. Rizzoli *et al.*, "Optimization of nonlinear microwave circuits by a harmonic-balance technique," in *Dig. IEE Colloquium CAD Microwave Circuits* (London), Nov. 1985, pp. 13/1–13/5.

[82] V. Rizzoli and C. Cecchetti, "Analysis of frequency-conversion effects in nonlinear microwave circuits," in *Proc. 1987 Microwave Symp./Brazil* (Rio de Janeiro), July 1987, pp. 1147–1154.

[83] S. A. Maas, "Two-tone intermodulation in diode mixers," *IEEE Trans. Microwave Theory Tech.*, vol. MTT-35, pp. 307–314, Mar. 1987.

[84] J. R. Mosig, "Accurate numerical techniques for characterization of microstrip structures and discontinuities," presented at the Workshop on Present Trends in Microwave CAD, Baltimore, June 5, 1986.

[85] Y. L. Chow *et al.*, "A modified moment method for the computation of complex MMIC circuits," in *Proc. 16th European Microwave Conf.* (Dublin), Sept. 1986, pp. 625–630.

[86] G. Ioos and D. D. Joseph, *Elementary Stability and Bifurcation Theory*. New York: Springer-Verlag, 1980.

[87] K. Kurokawa, "Some basic characteristics of broadband negative-resistance oscillator circuits," *Bell Syst. Tech. J.*, vol. 48, pp. 1937–1955, July–Aug. 1969.

[88] C. A. Brackett, "Characterization of second-harmonic effects in IMPATT diodes," *Bell Syst. Tech. J.*, vol. 49, pp. 1777–1810, Oct. 1970.

[89] G. H. B. Hansson and K. J. Lundström, "Stability criteria for phase-locked oscillators," *IEEE Trans. Microwave Theory Tech.*, vol. MTT-20, pp. 641–645, Oct. 1972.

[90] M. E. Hines, "Large-signal noise, frequency conversion and parametric instabilities in IMPATT diode networks," *Proc. IEEE*, vol. 60, pp. 1534–1548, Dec. 1972.

[91] J. Gonda and W. E. Schroeder, "IMPATT diode circuit design for parametric stability," *IEEE Trans. Microwave Theory Tech.*, vol. MTT-25, pp. 343–352, May 1977.

[92] R. Knöchel, "Unified large-signal stability and noise theory for syncronized oscillators," in *Proc. Inst. Elec. Eng.*, pt. H, vol. 128, pp. 137–145, June 1981.

[93] E. F. Calandra and A. M. Sommariva, "Stability analysis of injection locked oscillators in their fundamental mode of operation," *IEEE Trans. Microwave Theory Tech.*, vol. MTT-29, pp. 1137–1144, Nov. 1981.

[94] V. Rizzoli and A. Lipparini, "General stability analysis of periodic steady-state regimes in nonlinear microwave circuits," *IEEE Trans. Microwave Theory Tech.*, vol. MTT-33, pp. 30–37, Jan. 1985.

[95] A. I. Mees, "Limit cycle stability," *Journal I.M.A.*, vol. 11, pp. 281–295, 1973.
[96] D. J. Allwright, "Harmonic balance and the Hopf bifurcation," *Math. Proc. Camb. Phil. Soc.*, vol. 82, pp. 453–467, 1977.
[97] J. J. Di Stefano, A. R. Stublerud, and I. J. Williams, *Feedback and Control Systems*. Los Angeles: McGraw-Hill, 1967.
[98] V. Rizzoli and A. Neri, "Global stability analysis of microwave circuits by a frequency-domain approach," in *1987 IEEE MTT-S Int. Microwave Symp. Dig.* (Las Vegas), June 1987, pp. 689–692.
[99] H. Kawakami, "Bifurcation of periodic responses in forced dynamic nonlinear circuits: Computation of bifurcation values of the system parameters," *IEEE Trans. Circuits Syst.*, vol. CAS-31, pp. 248–260, Mar. 1984.
[100] A. I. Mees and L. O. Chua, "The Hopf bifurcation theorem and its applications to nonlinear oscillations in circuits and systems," *IEEE Trans. Circuits Syst.*, vol. CAS-26, pp. 235–254, Apr. 1979.
[101] M. I. Sobhy *et al.*, "The design of microwave monolithic voltage-controlled oscillators," in *Proc. 15th European Microwave Conf.* (Paris), Sept. 1985, pp. 925–930.
[102] K. Kurokawa, "Noise in syncronized oscillators," *IEEE Trans. Microwave Theory Tech.*, vol. MTT-16, pp. 234–240, Apr. 1968.
[103] R. D. Kuvås, "Nonlinear noise theory for IMPATT diodes," *IEEE Trans. Electron Devices*, vol. ED-23, pp. 395–411, 1976.
[104] K. F. Schunemann and K. Behm, "Nonlinear noise theory for synchronized oscillators," *IEEE Trans. Microwave Theory Tech.*, vol. MTT-27, pp. 452–458, May 1979.
[105] R. A. Pucel and J. Curtis, "Near-carrier noise in FET oscillators," in *1983 IEEE MTT-S Int. Microwave Symp. Dig.* (Boston), June 1983, pp. 282–284.
[106] B. T. Debney and J. S. Joshi, "A theory of noise in GaAs FET microwave oscillators and its experimental verification," *IEEE Trans. Electron Devices*, vol. ED-30, pp. 769–776, July 1983.
[107] G. K. Tie and C. S. Aitchinson, "Noise figure and associated conversion gain of a microwave MESFET gate mixer," in *Proc. 13th European Microwave Conf.* (Nürnberg), Sept. 1983, pp. 579–584.
[108] H. Rohdin, C. Yi, and C. Stolte, "A study of the relation between device low-frequency noise and oscillator phase noise for GaAs MESFETs," in *1984 IEEE MTT-S Int. Microwave Symp. Dig.* (San Francisco), June 1984, pp. 267–269.
[109] B. Villeneuve *et al.*, "RF spectrum of thermal noise and frequency stability of a microwave cavity-oscillator," *IEEE Trans. Microwave Theory Tech.*, vol. MTT-32, pp. 1565–1572, Dec. 1984.
[110] H. J. Siweris and B. Schiek, "Analysis of noise upconversion in microwave FET oscillators," *IEEE Trans. Microwave Theory Tech.*, vol. MTT-33, pp. 233–242, Mar. 1985.
[111] H. J. Siweris and B. Schiek, "A GaAs FET oscillator noise model with a periodically driven noise source," in *Proc. 16th European Microwave Conf.* (Dublin), Sept. 1986, pp. 681–686.
[112] J. M. Bunting, M. J. Howes, and J. R. Richardson, "Large-signal time-domain modelling of noise in the design of MESFET oscillators," in *Proc. 16th European Microwave Conf.* (Dublin), Sept. 1986, pp. 201–206.
[113] C. Dragone, "Analysis of thermal and shot noise in pumped resistive diodes," *Bell. Syst. Tech. J.*, vol. 47, pp. 1883–1902, Nov. 1968.
[114] V. Rizzoli and A. Lipparini, "Computer-aided noise analysis of linear multiport networks of arbitrary topology," *IEEE Trans. Microwave Theory Tech.*, vol. MTT-33, pp. 1507–1512, Dec. 1985.
[115] H. Fukui, Ed., *Low-Noise Microwave Transistors & Amplifiers*. New York: IEEE Press, 1981.
[116] K. Hwang, Ed., *Supercomputers: Design and Applications*. Silver Springs, MD: IEEE Computer Society Press, 1984.
[117] J. T. Devreese and P. Van Camp, Eds., *Supercomputers in Theoretical and Experimental Science*. New York: Plenum Press, 1985.
[118] K. Hwang *et al.*, "Vector computer architecture and processing techniques," *Advances in Comput.*, vol. 20, pp. 115–197.
[119] R. W. Hockney and C. R. Jesshope, *Parallel Computers*. Bristol: Adam Hilger Ltd., 1981.
[120] L. Nelson and P. Rigsbee, "Multitasking at Cray," *CRAY CHANNELS*, vol. 7, pp. 12–15, Summer 1985.
[121] M. Booth and K. Misegades, "Microtasking: A new way to harness multiprocessors," *CRAY CHANNELS*, vol. 8, pp. 24–27, Summer 1986.
[122] V. Rizzoli and M. Ferlito, "Vector processing concepts in microwave circuit design," in *Proc. 14th European Microwave Conf.* (Liège), Sept. 1984, pp. 847–852.
[123] V. Rizzoli, M. Ferlito, and A. Neri, "Vectorized program architectures for supercomputer-aided circuit design," *IEEE Trans. Microwave Theory Tech.*, vol. MTT-34, pp. 135–141, Jan. 1986.

✠

Vittorio Rizzoli (M'79) was born in Bologna, Italy, in 1949. He graduated from the School of Engineering, University of Bologna, in July 1971.

From 1971 to 1973, he was with the Centro Onde Millimetriche of Fondazione Ugo Bordoni, Pontecchio Marconi, Italy, where he was involved in research on millimeter-waveguide communication systems. In 1973, he was with the Hewlett-Packard Company, Palo Alto, CA, working in the areas of MIC and microwave power devices. From 1974 to 1979, he was an Associate Professor at the University of Bologna, teaching a course on microwave integrate circuits. In 1980, he joined the University of Bologna as a full Professor of Electromagnetic Fields and Circuits. His current research interests are in the fields of MIC and MMIC, with special emphasis on nonlinear circuits. He is also heading a research project aimed at the development of vectorized software for microwave circuit design applications.

✠

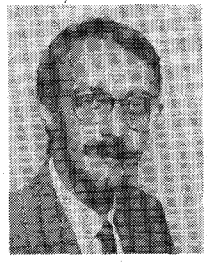

Andrea Neri was born in Bologna, Italy, in 1957. He graduated in electronic engineering from the University of Bologna in July 1981.

In 1983 and 1984, he obtained research grants issued by Fondazione G. Marconi, Pontecchio Marconi, Italy, and Selenia S.p.A., Rome, Italy, to work on dielectric resonators and their applications in MIC. In 1985, he joined Fondazione U. Bordoni, Rome, Italy, where he is currently involved in research on nonlinear microwave circuit design. His main fields of interest are the characterization of microwave components by means of electromagnetic methods and the application of supercomputers in MIC and MMIC design.